1963

The dynamic response of flow forced heat exchangers

Franklin Joe Stermole
Iowa State University

THE DYNAMIC RESPONSE OF FLOW FORCED HEAT EXCHANGERS

by

Franklin Joe Stermole

A Dissertation Submitted to the
Graduate Faculty in Partial Fulfillment of
The Requirements for the Degree of
DOCTOR OF PHILOSOPHY

Major Subject: Chemical Engineering

Approved:

Signature was redacted for privacy.

In Charge of Major Work

Signature was redacted for privacy.

Head of Major Department

Signature was redacted for privacy.

Dean of Graduate College

Iowa State University
Of Science and Technology
Ames, Iowa

1963

TABLE OF CONTENTS

ABSTRACT

The purpose of this investigation was to study both experimentally and theoretically the dynamic response of a double pipe counter-current heat exchanger subjected to flow rate changes in order to develop mathematical models that adequately describe the dynamics of this distributed parameter system. An insulated heat exchanger 14.7 feet long was constructed using a 1 inch nominal type K copper pipe placed concentrically inside a 2 inch nominal schedule 40 iron pipe shell.

Experimental data for both large and small flow perturbations about a mean flow rate gave the same frequency response curves, indicating the system behaves linearly with respect to flow upsets in the flow range investigated. The effects of wall capacitance and heat transfer coefficient variation were found to have little effect on normalized frequency response results, but variation of the heat transfer coefficient contributed significantly to transient response results. Partial differential equation models with constant coefficients gave good agreement with experimental frequency response results over all frequencies tested, but only agreed with experimental transient results for small flow upsets. Ordinary differential equation models with variable coefficients represented the transient response of

the system satisfactorily for both large and small upsets, but represented the frequency response adequately only at low frequencies. Experimental frequency response resonance occurred when $L\omega/V = 2\pi$, where L equals heat exchanger length, ω equals upset frequency and V is the mean velocity of fluid having its temperature response measured.

INTRODUCTION

For linear processes, frequency response data can assist in the design of process systems as described in Smith (21) and Wilt (25). Because heat exchangers are of such wide use in the chemical industry, study of their response to flow rate upsets is justified on the basis of industrial importance alone. Simplified transfer functions that are solvable by hand calculation methods and that accurately represent specific distributed parameter heat exchange processes are needed to eliminate the need for costly and time consuming frequency response measurements which must now be made experimentally or predicted on a digital computer using complex programs.

Study of a simple concentric double pipe heat exchanger permits a close look at the fundamental heat transfer process and enables one to attach relative significance to various terms in the mathematical description of the specified process. This permits elimination of mathematical terms that complicate a theoretical description of the process but add little to its accuracy.

Counter-current processes are used extensively in engineering work. They provide in general the maximum difference in potential for a transport process taking place between two fluid streams. Extraction columns, distillation

columns, absorption columns and tubular flow reactors are typical examples of processes that behave similarly to counter-current heat exchangers. To design an adequate control system for such processes, the dynamics of the process must be known, and it must be known in a form that is understandable and useable by engineers in industry.

The purpose of this investigation was to study the dynamics of concentric double pipe heat exchangers subjected to flow rate perturbations, with primary emphasis being given to counter-current heat exchange. The main approaches presented in this study are frequency and transient response analysis, which effectually test the hypothesis that a heat exchanger behaves as a linear system with respect to flow disturbances. Experimentally corroborated theoretical models of counter-current heat exchangers are presented. The heat exchange results obtained in this investigation are representative of a wide range of distributed parameter processes and form the basis for study of the more complicated processes.

LITERATURE SURVEY

The literature concerning flow-forced heat exchangers is limited. Temperature-forced heat exchange processes have been studied to a greater extent because dynamic equations describing heat exchangers for temperature upsets have constant coefficients and are easier to solve than the variable coefficient equations that result from flow upsets. Techniques for obtaining temperature-forced transfer functions are often similar, however, to those that permit determination of flow-forced transfer functions. Therefore, although this project is concerned primarily with flow upsets in double pipe heat exchangers, it is beneficial to survey the literature concerning both flow and temperature upsets to heat exchange processes.

Hempel (12) derived transfer function models of a steam-water heat exchange system for upsets in steam temperature, water flow rate or input temperature. Tube wall capacitance and heat transfer coefficient variation were considered. Comparison of experimental and theoretical frequency response results was good and the distributed parameter property of resonance was predicted. Koppel (14) obtained a model for the dynamics of a steam-water heat exchanger by applying the method of characteristic equations to a partial differential equation representation of the

system. Theoretical results were given for transient response, but no comparison was made with experimental results. Lees and Hougen (15) pulse-tested the flow rate of a steam-water heat exchanger and converted the experimental wave forms to frequency response results using Fourier transformation theory with the aid of a digital computer. No attempt was made to obtain a theoretical representation of the system. Stermole (22) and Stermole and Larson (23) investigated flow upsets of a steam-water heat exchanger using ordinary differential equation models. Transient and frequency response for theoretical and experimental data were in good agreement. A partial differential equation model which neglected tube wall capacitance was solved for flow-forced frequency response and shown to give good agreement with experimental data. Resonance was shown to occur when $\frac{L\omega}{V} = 2\pi$, where L = heat exchanger length, ω = upset frequency and V = mean fluid velocity for either flow rate or temperature upsets.

Fanning (8) investigated the dynamics of a continuous agitated-tank exchanger to upsets in flow rate and temperature. Ordinary differential equation models of the system were solved and compared with experimental frequency and transient response data. Mozely (17) presented one of the first lumped parameter representations of double pipe heat exchangers to appear in the literature. Assuming perfectly

mixed fluid in both the shell and tube, with bulk temperature equal to exit temperature, the following differential equations were presented:

$$\frac{M_s}{W_s}\frac{d\theta_s}{d+} + \theta_s + \frac{UA}{W_s C_s}(\theta_s - \theta_t) = \theta_{s\ in}$$

$$\frac{M_t}{W_t}\frac{d\theta_t}{dt} + \theta_t + \frac{UA}{W_t C_t}(\theta_t - \theta_s) = \theta_{t\ in}$$

M represents mass holdup of fluid in tube or shell, W is mass flow rate, C is heat capacity, and other symbols are consistent with the nomenclature. Transfer functions were obtained from these equations for tube temperature forced by input temperature of either fluid and for tube temperature forced by the flow rate of either fluid. The temperature forced models were checked with experimental data but the flow-forced models were not compared with experimental data. For temperature upsets a model was also derived for arithmetic average temperature in the shell and tube, but this was not done for flow upsets.

Edwards' dissertation (6) contains a treatment of the derivation of flow-forced transfer functions in compact matrix notation for counter-current heat exchange. They are in good form for digital computer solution. Comparison of

theoretical and experimental frequency response results was good, but the distributed parameter resonance effect was not observed experimentally or predicted theoretically. Experimental frequency response data were obtained by applying harmonic analysis to actual waveforms that resulted from pulsing input flow rates.

Takahashi (24) presented one of the first published papers concerning the theory of basic transfer functions for a temperature forced heat exchanger represented by partial differential equations. He considered four cases: (a) both fluids unmixed, (b) one fluid unmixed, (c) both fluids mixed, and (d) percolation, i.e., one fluid flowing along a solid surface. Paynter and Takahashi (18) modified this conventional approach by presenting a new method of evaluating dynamic response based on an analogy between statistical measures and heat exchange parameters.

Campbell (1) gave a transfer function obtained from the partial differential equations representing two fluid double pipe heat exchangers for temperature upsets. The partial differential equations were reduced to complex double transformed transfer functions but are not in a form that can be solved easily. Iscol (13) reduced these equations to a compact matrix notation and obtained a digital computer frequency response solution that was compared with experimental frequency response data obtained by applying harmonic

analysis to experimental waveforms resulting from pulsations of the input temperature. Gilliland, Gould and Rinard (10) derived transfer functions for temperature upsets from these same partial differential equations by utilizing a Nuemann series approximation. Experimental data were not utilized to check this method, but both transient and frequency response theory were discussed. The resulting transfer functions were complex but could still be solved by hand calculations. Future application of this technique to flow upsets should be a worthwhile study to undertake. Morris (16) predicted outlet temperature response to inlet temperature disturbances in a two-fluid exchanger using a digital computer to facilitate frequency response calculations. Theoretical results agreed favorably with experimental frequency results obtained from pulse test data using the method of Lees and Hougen (15).

Cohen and Johnson (4) presented a transfer function that described the dynamics of a steam-water heat exchanger very satisfactorily for steam temperature upsets. The distributed parameter phenomenon of resonance that had been observed earlier by Debolt (5) was predicted. Debolt's study was also concerned with steam temperature upsets, but he used lumped parameter models and did not predict resonance although he was one of the early experimental observers of this effect. Debolt also represented his system with an

electrical analog system. Cima and London (3) also used the electrical analog technique to predict transient response in a two-fluid counterflow gas turbine regenerator. Ford (9) used electrical analogs to represent the dynamics of steam-water heat exchangers to variations in inlet fluid temperature.

Rizika (19, 20) considered two fluid heat exchangers in general. In the first paper (19) Rizika formulated the generalized equations of performance of two-fluid systems, analyzed them using Laplace transform theory, and obtained theoretical transfer functions. The solutions were expressed in terms of complex mathematical expressions. Transient response was predicted for input temperature upsets. The second paper (20) was concerned with an extension of this work as an application to the incompressible fluid case. Yang, Clark, and Arpaci (26) studied the dynamics of heat exchangers having heat sources in the walls. Complex transfer functions for wall temperature upsets were solved for transient and frequency analysis with the aid of a digital computer.

Fanning (7) analyzed automatic control loops in a plant, utilizing a simple steam-water heat exchanger subjected to steam temperature upsets. An ordinary differential equation model of the process was found to be adequate for this study. Hainsworth, Tivy and Paynter (11) used a commercial

shell and tube steam-water heat exchanger to study lags due to transmission lines and temperature sensing elements. An electrical analog simulation of the process was used to study optimum controller settings for different forms of temperature sensing elements and different lengths of pneumatic transmission lines.

MATHEMATICAL DEVELOPMENT

A mathematical description of a distributed parameter double pipe heat exchanger with fluid flowing in both the shell and tube may be obtained from heat balances over both fluid phases and the metal wall. The resulting equations for counter-current heat exchange are:

$$\frac{\partial \theta_s}{\partial t} - V_s \frac{\partial \theta_s}{\partial x} = \frac{h_s P_s}{\rho_s A_s C_s} (\theta_w - \theta_s) \qquad \text{(Eq. 1)}$$

$$\frac{\partial \theta_t}{\partial t} + V_t \frac{\partial \theta_t}{\partial x} = \frac{h_t P_t}{\rho_t A_t C_t} (\theta_w - \theta_t) \qquad \text{(Eq. 2)}$$

$$\frac{\partial \theta_w}{\partial t} = \frac{h_s P_s}{\rho_w A_w C_w} (\theta_s - \theta_w) + \frac{h_t P_t}{\rho_w A_w C_w} (\theta_t - \theta_w) \qquad \text{(Eq. 3)}$$

These equations are based on the following assumptions:

1. Fluid temperatures and velocities are uniform across the cross section normal to the direction of flow, i.e., well developed turbulent flow.
2. Thermal conductivity of the inner pipe wall is infinite in the radial direction and heat

conduction in the axial direction is negligible, a condition valid for thin metallic walls.

3. Liquid water is incompressible and its specific heat and density are constant.
4. Axial heat conduction in the fluids is negligible compared to heat transported by bulk flow.
5. Shell wall dynamics may be neglected.

The direction of flow of tube fluid has been taken in the same direction as the coordinate system. These equations are identical to those that describe a co-current flow heat exchanger except for the negative sign on the term involving V_s in Equation 1. This term is negative for counter-current flow because V_s flows in the opposite direction of the coordinate system for heat exchanger length. This makes application of the boundary conditions more complicated for counter-current flow than for co-current flow as will be shown later.

Starting with Equations 1, 2, and 3, several mathematical models have been developed to relate output tube fluid temperature to shell and tube flow rate upsets. Development of these models was directed toward studying the effects of tube wall capacitance, heat transfer coefficient variation and lumped parameter representation of the distributed parameter system in an effort to satisfactorily

represent the flow forced heat exchange system with the simplest model possible. Both transient and frequency flow rate upsets were used to test the models against experimental data.

The derivation is presented for upsets in either the shell or tube flow rate in a form that permits obtaining transfer functions for either V_t or V_s forcing θ_t. These transfer functions can then be solved for frequency response amplitude ratios and phase lags by letting the Laplace transform variable s equal iw. Transient response data can be obtained by inverting the transfer functions into real time and solving analytically for θ_{tL} at different times.

Model Including Wall Capacitance

Derivation of the transfer function $\overline{\theta}_t/\overline{V}_t$ from Equations 1, 2, and 3 will now be shown. For flow rate disturbances, Equations 1, 2, and 3 must be reduced to constant coefficient equations to permit application of standard Laplace transformation techniques to obtain desired transfer functions. This is accomplished by letting θ_t, θ_s, θ_w, V_t, V_s, B_t, B_s, B_3, and B_4 be expressed as the sum of a steady state value and a perturbation from steady state, where

$$B_t = \frac{h_t P_t}{\rho_t A_t C_t},\ B_s = \frac{h_s P_s}{\rho_s A_s C_s},\ B_3 = \frac{h_t P_t}{\rho_w A_w C_w},\ B_4 = \frac{h_s P_s}{\rho_w A_w C_w}$$

$$\theta_t = \theta_{ti} + \theta_t',\ \theta_s = \theta_{si} + \theta_s',\ \theta_w = \theta_{wi} + \theta_w'$$

$$V_t = V_{ti} + V_t',\ V_s = V_{si} + V_s',\ B_t = B_{ti}\left(1 + \frac{k_t V_t'}{V_{ti}}\right)$$

$$B_s = B_{si}\left(1 + \frac{k_s V_s'}{V_{si}}\right),\ B_3 = B_{3i}\left(1 + \frac{k_s V_s'}{V_{si}}\right),\ B_4 = B_{4i}\left(1 + \frac{k_t V_t'}{V_{ti}}\right)$$

Substitution into Equations 1, 2, and 3 and dropping the terms involving the product of two perturbations gives the equations in terms of steady state and dynamic quantities. At steady state,

$$-V_{si}\frac{d\theta_{si}}{dx} = B_{si}(\theta_{wi} - \theta_{si}) \qquad \text{(Eq. 1a)}$$

$$+V_{ti}\frac{d\theta_{ti}}{dx} = B_{ti}(\theta_{wi} - \theta_{ti}) \qquad \text{(Eq. 2a)}$$

$$0 = B_{3i}(\theta_{si} - \theta_{ti}) + B_{4i}(\theta_{ti} - \theta_{wi}) \qquad \text{(Eq. 3a)}$$

Subtraction of the steady state equations from the

total equations yields the following dynamic equations:

$$\frac{\partial \theta_s'}{\partial t} - V_{si}\frac{\partial \theta_s'}{\partial x} - V_s'\frac{\partial \theta_{si}}{\partial x} = B_{si}k_s(\theta_{wi}-\theta_{si})\frac{V_s'}{V_{si}} + B_{si}(\theta_w'-\theta_s') \qquad \text{(Eq. 1b)}$$

$$\frac{\partial \theta_t'}{\partial t} + V_{ti}\frac{\partial \theta_t'}{\partial x} + V_t'\frac{\partial \theta_{ti}}{\partial x} = B_{ti}k_t(\theta_w-\theta_{ti})\frac{V_t'}{V_{ti}} + B_{ti}(\theta_w'-\theta_t') \qquad \text{(Eq. 2b)}$$

$$\frac{\partial \theta_w'}{\partial t} + (B_{3i} + B_{wi})\,\theta_w' = B_{3i}k_s(\theta_{si}-\theta_{wi})\frac{V_s'}{V_{si}} + B_{4i}k_t(\theta_{ti}-\theta_{wi})\frac{V_t'}{V_{ti}}$$

$$+ B_{3i}\theta_s' + B_{4i}\theta_t' \qquad \text{(Eq. 3b)}$$

The steady state Equations 1a, 2a, and 3a can be combined and solved to obtain θ_{ti} and θ_{si} which may then be differentiated to give:

$$\frac{\partial \theta_{ti}}{\partial x} = \frac{(\theta_{tLi} - \theta_{tOi})}{e^{m_1 L} - 1}\, m_1 e^{m_1 x}$$

$$\frac{\partial \theta_{si}}{\partial x} = \frac{(\theta_{sLi} - \theta_{sOi})}{e^{m_1 L} - 1}\, m_1 e^{m_1 x}$$

where

$$m_1 = \frac{V_{ti}B_{si}B_{4i} - V_{si}B_{ti}B_{3i}}{V_{ti}V_{si}(B_{3i} + B_{4i})}$$

m_1 is a root of the second order steady state equation for both θ_{si} and θ_{ti}. The other root is zero in both cases. However, the steady state solution for θ_{si} and θ_{ti} are different even though the roots are equal because the boundary condition are different. For the shell, $\theta_{si} = \theta_{sLi}$ at $x = L$ and $\theta_{si} = \theta_{sOi}$ at $x = 0$. For the tube $\theta_{ti} = \theta_{tLi}$ at $x = L$ and $\theta_{ti} = \theta_{tOi}$ at $x = 0$.

Upon substitution for $\partial\theta_{ti}/\partial x$ and $\partial\theta_{si}/\partial x$ in Equations 1b and 2b, it is evident that Equations 1b, 2b, and 3b are linear and have constant coefficients with respect to time on all forcing and dependent variables. Laplace transformation can now be utilized to obtain transfer functions for the shell or tube fluid temperature forced by upsets in either fluid flow rate. Transfer functions for temperature upsets could also be obtained from these equations. However, this study considers only the effect of flow perturbations. Transformation of Equations 1b, 2b, and 3b with respect to time, the elimination of $\bar{\theta}_w$ from the transformed equations and rearrangement yields the following two equations for a tube flow upset with a constant shell flow rate:

$$\frac{d\overline{\theta}_s}{dx} - a_1\overline{\theta}_s = g_1\overline{V}_t + h_1\overline{V}_t e^{m_1 x} - f_1\overline{\theta}_t \qquad \text{(Eq. 1c)}$$

$$\frac{d\overline{\theta}_t}{dx} + a_2\overline{\theta}_t = g_2\overline{V}_t + h_2\overline{V}_t e^{m_1 x} + f_2\overline{\theta}_s \qquad \text{(Eq. 2c)}$$

where

$$a_1 = \frac{(s + B_{si})(s + B_{3i} + B_{4i}) - B_{si}B_{3i}}{V_{si}(s + B_{3i} + B_{4i})},$$

$$a_2 = \frac{(s + B_{ti})(s + B_{3i} + B_{4i}) - B_{ti}B_{4i}}{V_{ti}(s + B_{3i} + B_{4i})},$$

$$g_1 = \frac{B_{si}B_{4i}B_{3i}k_t\{(\theta_{t0i} - \theta_{s0i})e^{m_1 L} + \theta_{sLi} - \theta_{tLi}\}}{V_{si}V_{ti}(s + B_{3i} + B_{4i})(B_{3i} + B_{4i})(1 - e^{m_1 L})},$$

$$f_1 = \frac{B_{si}B_{4i}}{V_{si}(s + B_{3i} + B_{4i})},$$

$$h_1 = \frac{B_{si}B_{4i}B_{3i}k_t(\theta_{tLi} - \theta_{t0i} - \theta_{sLi} + \theta_{s0i})}{V_{si}V_{ti}(s + B_{3i} + B_{4i})(B_{3i} + B_{4i})(1 - e^{m_1 L})},$$

$$f_2 = \frac{B_{ti}B_{3i}}{V_{ti}(s + B_{3i} + B_{4i})},$$

$$g_2 = [B_{ti}k_t - \frac{B_{ti}B_{4i}k_t}{s + B_{3i} + B_{4i}}][\frac{B_{3i}}{(B_{3i} + B_{4i})(1 - e^{m_1 L})}]$$

$$[\frac{(\theta_{t0i} - \theta_{s0i})e^{m_1 L} + \theta_{sLi} - \theta_{tLi}}{V_{ti}^2}],$$

$$h_2 = [\frac{\theta_{tLi} - \theta_{t0i}}{1 - e^{m_1 L}}]\frac{m_1}{V_{ti}} + g_2[\frac{\theta_{tLi} - \theta_{t0i} - \theta_{sLi} + \theta_{s0i}}{(\theta_{t0i} - \theta_{s0i})e^{m_1 L} + \theta_{sLi} - \theta_{tLi}}]$$

Transforming Equations 1c and 2c with respect to x gives

$$(p - a_1)\bar{\bar{\theta}}_s + f_1\bar{\bar{\theta}}_t = (\frac{g_1}{p} + \frac{h_1}{p - m_1})\bar{V}_t + \bar{\theta}_{s0} \qquad \text{(Eq. 1d)}$$

$$- f_2\bar{\bar{\theta}}_s + (p + a_2)\bar{\bar{\theta}}_t = (\frac{g_2}{p} + \frac{h_2}{p - m_1})\bar{V}_t \qquad \text{(Eq. 2d)}$$

The boundary conditions are $\bar{\theta}_s = \bar{\theta}_{s0}$ and $\bar{\theta}_t = \bar{\theta}_{t0}$ at $x = 0$. For constant input tube fluid temperature $\bar{\theta}_{t0}$ is zero, but $\bar{\theta}_{s0}$ is output shell temperature and consequently varies with time. For co-current flow both boundary conditions would be zero and therefore the co-current system yields a simpler mathematical description than a counter-current system. The coefficients of all terms in Equations 1c and 2c are functions of transformed time only. Therefore

these equations may be solved for the transfer function $\overline{\theta}_t/\overline{V}_t$ by transforming them a second time with respect to the length variable x and then eliminating $\overline{\overline{\theta}}_s$ by combining the two equations and inverting back to the x domain. However, the resulting transfer function is extremely long and complex and of questionable practical value. In an effort to obtain the transfer function in a more useable form, the significance of each term in Equation 2c was investigated. Temperature of the tube fluid is being forced by the change in flow rate of the tube fluid and by the temperature change of shell fluid. Comparison of the magnitude of these forcing terms using experimental data shows that for equal mass flow rates in the shell and tube the temperature forcing term is about seven per cent as large as the flow forcing terms. For mass flow rates in the shell greater than in the tube, the effect of shell temperature change is proportionately less until at infinite shell flow rates the shell temperature remains constant and contributes nothing to the dynamics of flow upsets. The infinite shell flow rate case is analogous to a steam jacketed heat exchanger in that shell temperature remains constant. For all these cases, when flow upsets occur the change in residence time of the fluid and heat transfer coefficient variation are more important considerations than change in shell temperature. Neglecting the temperature forcing term involving $\overline{\theta}_s$

in Equation 2c results in the following transfer function:

$$\frac{\bar{\theta}_{tL}}{\bar{V}_t} = \frac{h_2}{m_1 + a_2}\left(e^{m_1 L} - e^{-a_2 L}\right) + \frac{g_2}{a_2}\left(1 - e^{-a_2 L}\right) \qquad \text{Model I}$$

The g_2 term of Model I is directly dependent upon heat transfer coefficient variation. Referring to the defining equation for g_2, if the tube side heat transfer film coefficient is considered constant, $k_t = 0$ and therefore $g_2 = 0$. Only part of h_2 is dependent upon heat transfer coefficient variation, therefore, it has a finite value for tube flow upsets when the heat transfer coefficient is considered constant. Therefore, for constant heat transfer coefficients:

$$\frac{\bar{\theta}_{tL}}{\bar{V}_L} = \frac{h_2}{m_2 + a_2}\left(e^{m_1 L} - e^{-a_2 L}\right) \qquad \text{Model II}$$

Models Neglecting Wall Capacitance

If the tube wall capacitance is considered to be negligible, the left side of Equation 3 is equal to zero. Combining Equations 1, 2, and 3 to eliminate the tube wall temperature gives the following two partial differential equations with an overall heat transfer coefficient.

$$\frac{\partial \theta_s}{\partial t} - V_s \frac{\partial \theta_s}{\partial x} = K_s(\theta_t - \theta_s) \qquad \text{(Eq. 4)}$$

$$\frac{\partial \theta_t}{\partial t} + V_t \frac{\partial \theta_t}{\partial x} = K_t(\theta_s - \theta_t) \qquad \text{(Eq. 5)}$$

where

$$K_s = \frac{UP_t}{\rho_s A_s C_{ps}} \text{ and } K_t = \frac{UP_t}{\rho_t A_t C_{pt}}$$

Transfer functions for $\overline{\theta}_t/\overline{V}_t$ and $\overline{\theta}_t/\overline{V}_s$ can be derived from Equations 4 and 5 by utilizing the same procedure used to develop Model I. These same transfer functions can also be used to represent shell temperature forced by upsets in either flow rate by properly changing the subscript nomenclature, i.e., by interchanging shell and tube parameters and variables in the equations. The overall heat transfer coefficient is considered to vary directly with upsets in either fluid flow rate. The temperature and flow rate variables are expressed as the sum of steady state and perturbation values as previously defined.

$$K_s = K_{si}\left(1 + \frac{k_s V_s'}{V_{si}} + \frac{k_t V_t'}{V_{ti}}\right), \quad K_t = K_{ti}\left(1 + \frac{k_s V_s'}{V_{si}} + \frac{k_t V_t'}{V_{ti}}\right)$$

Substituting the new variables into Equations 4 and 5, dropping the products of perturbations, subtracting the steady state equations and substituting for $\partial\theta_{ti}/\partial x$ and $\partial\theta_{si}/\partial x$ from the solutions of the steady state equations gives the following dynamic equations:

$$\frac{\partial\theta_s'}{\partial t} - \frac{(\theta_{sLi} - \theta_{sOi})}{e^{m_2 L} - 1} m_2 e^{m_2 x} V_s' - V_{si}\frac{\partial\theta_s'}{\partial x} = K_{si}(\theta_t' - \theta_s')$$

$$+ K_{si}(C + De^{m_2 x})\left(\frac{k_s V_s'}{V_{si}} + \frac{k_t V_t'}{V_{ti}}\right) \qquad \text{(Eq. 4a)}$$

$$\frac{\partial\theta_t'}{\partial t} + \frac{(\theta_{tLi} - \theta_{tOi})}{e^{m_2 L} - 1} m_2 e^{m_2 x} V_t' + V_{ti}\frac{\partial\theta_t'}{\partial x} = K_{ti}(\theta_s' - \theta_t')$$

$$- K_{ti}(C + De^{m_2 x})\left(\frac{k_s V_s'}{V_{si}} + \frac{k_t V_t'}{V_{ti}}\right) \qquad \text{(Eq. 5a)}$$

where

$$m_2 = \frac{K_{si}}{V_{si}} - \frac{K_{ti}}{V_{ti}}$$

$$C = \frac{(\theta_{tOi} - \theta_{sOi})e^{m_2 L} - (\theta_{tLi} - \theta_{sLi})}{e^{m_2 L} - 1}$$

$$D = \frac{\theta_{tLi} - \theta_{sLi} - \theta_{t0i} + \theta_{s0i}}{e^{m_2 L} - 1}$$

After Laplace transformation with respect to time using the counter-current boundary conditions given previously, Equations 4a and 5a take the following form:

$$\frac{d\bar{\theta}_s}{dx} - \alpha_1 \bar{\theta}_s = -\frac{K_{si}}{V_{si}} \bar{\theta}_t - N_1 e^{m_2 x} \bar{V}_s - K_{si}(C + De^{m_2 x})$$

$$(\frac{k_s \bar{V}_s}{V_{si}} + \frac{k_t \bar{V}_t}{V_{ti}}) \qquad \text{(Eq. 4b)}$$

$$\frac{d\bar{\theta}_t}{dx} + \alpha_2 \bar{\theta}_t = \frac{K_{ti}}{V_{ti}} \bar{\theta}_s - N_2 e^{m_2 x} V_t' - K_{ti}(C + De^{m_2 x})$$

$$(\frac{k_s \bar{V}_s}{V_{si}} + \frac{k_t \bar{V}_t}{V_{ti}}) \qquad \text{(Eq. 5b)}$$

where

$$\alpha_1 = \frac{s + K_{si}}{V_{si}}, \qquad \alpha_2 = \frac{s + K_{ti}}{V_{ti}}$$

$$N_1 = (\frac{\theta_{sLi} - \theta_{s0i}}{e^{m_2 L} - 1})(\frac{m_2}{V_{si}}), \qquad N_2 = (\frac{\theta_{tLi} - \theta_{t0i}}{e^{m_2 L} - 1})(\frac{m_2}{V_{ti}})$$

Tube flow upset models

Neglecting the temperature forcing term involving $\bar{\theta}_s$ in Equation 5b, the following transfer function is obtained for tube flow rate forcing tube temperature with a constant shell flow rate.

$$\frac{\bar{\theta}_{tL}}{\bar{V}_t} = -\frac{(N_2 + R_2)}{m_2 + \alpha_2}\left(e^{m_2 L} - e^{-\alpha_2 L}\right) - \frac{Q_2}{\alpha_2}\left(1 - e^{-\alpha_2 L}\right) \quad \text{Model III}$$

where

$$R_2 = \frac{K_{ti} k_t D}{V_{ti}}, \qquad Q_2 = \frac{K_{ti} k_t C}{V_{ti}}$$

For a constant overall heat transfer coefficient, R_2 and Q_2 are zero because $k_t = 0$. Therefore, the model that results when a constant overall heat transfer coefficient is assumed is as follows:

$$\frac{\bar{\theta}_{tL}}{\bar{V}_t} = -\frac{N_2}{m_2 + \alpha_2}\left(e^{m_2 L} - e^{-\alpha_2 L}\right) \quad \text{Model IV}$$

For equal mass flow rates in the shell and tube, $m_2 = 0$ and Model IV reduces to

$$\frac{\overline{\theta}_{tL}}{\overline{V}_t} = \frac{-N_2}{\alpha_2}\left(1 - e^{-\alpha_2 L}\right) \qquad \text{(Eq. 6)}$$

For infinite shell flow rate (constant shell temperature), $m_2 = -K_{ti}/V_{ti}$ since $K_{si}/V_{si} = 0$. Therefore, for an infinite shell flow rate Model IV reduces to the same transfer function that is obtained for a steam-water heat exchanger forced by flow rate upsets as presented by Stermole and Larson (23).

$$\frac{\overline{\theta}_{tL}}{\overline{V}_t} = \frac{-N_2 V_{ti}}{s} e^{-\frac{K_{tiL}}{V_{ti}}}\left(1 - e^{-\frac{sL}{V_{ti}}}\right) \qquad \text{(Eq. 7)}$$

where

$$N_2 = \left(\frac{\theta_{tOi} - \theta_{tLi}}{e^{-\frac{K_{tiL}}{V_{ti}}} - 1}\right)\frac{K_{ti}}{V_{ti}^2}$$

Models III and IV are made applicable to co-current heat exchange by changing the sign of V_{si}, which appears only in m_2. Note that this yields a different limiting model for equal mass flow rates than the counter-current model because m_2 does not go to zero.

Summarizing, Models III and IV are applicable to

counter-current, co-current and constant shell temperature heat exchange when the correct value of m_2 is used for each case. Other parameters are the same for all cases. The differences in m_2 are summarized as follows:

counter-current, unequal mass flow rates, $m_2 = \frac{K_{si}}{V_{si}} - \frac{K_{ti}}{V_{ti}}$

counter-current, equal mass flow rates, $m_2 = 0$

co-current, unequal mass flow rates, $m_2 = -\frac{K_{si}}{V_{si}} - \frac{K_{ti}}{V_{ti}}$

co-current equal mass flow rates, $m_2 = -\frac{2K_{ti}}{V_{ti}}$

constant shell temperature (infinite shell flow), $m_2 = -\frac{K_{ti}}{V_{ti}}$

Shell flow upset model

It is shown later in the comparison of theoretical and experimental results that variation of the heat transfer coefficient has only a very small effect on frequency response results using Models I through IV. Because the model for shell flow upsets forcing tube temperature is more complex than the tube flow forcing models and since neglecting the heat transfer coefficient variation gives a significantly

simpler model without greatly reducing the accuracy of frequency response results, a constant overall heat transfer coefficient was assumed for the derivation of the $\overline{\theta}_t/\overline{V}_s$ transfer function. The derivation of this model from Equations 4b and 5b can be conducted using the same procedure employed to obtain Model IV. However, a simple series approximation solution can be employed to obtain both $\overline{\theta}_t/\overline{V}_s$ and $\overline{\theta}_t/\overline{V}_t$. This method was used by Gilliland, Gould and Rinard (10) for temperature upsets in a double pipe heat exchanger. It shows that the first term in the series representation of either $\overline{\theta}_t/\overline{V}_t$ or $\overline{\theta}_t/\overline{V}_s$ neglects the temperature forcing term in the equation for the fluid that is upset, and that in fact the same transfer functions result that are obtained by neglecting these temperature terms in Equation 4b and Equation 5b and using the double transformation derivation previously described. While the approximation that results in Model IV is due to neglecting the $\overline{\theta}_s$ temperature forcing term in Equation 5b, the approximation that yields the $\overline{\theta}_t/\overline{V}_s$ transfer function is due to neglecting the $\overline{\theta}_t$ temperature forcing term in Equation 4b.

For a constant overall heat transfer coefficient, Equations 4b and 5b are integrated individually with the boundary conditions $\overline{\theta}_{t0} = 0$ and $\overline{\theta}_{sL} = 0$.

$$e^{-\alpha_1 x}\,\bar{\theta}_s\Big|_x^L = -\frac{K_{si}}{V_{si}}\int_x^L e^{-\alpha_1 x}\,\bar{\theta}_t dx - N_1\int_x^L e^{(m_2-\alpha_1)x}\,\bar{V}_s dx$$

$$e^{+\alpha_2 x}\,\bar{\theta}_t\Big|_0^x = +\frac{K_{ti}}{V_{ti}}\int_0^x e^{+\alpha_2 x}\,\bar{\theta}_s dx - N_2\int_0^x e^{(m_2+\alpha_2)x}\,\bar{V}_t dx$$

Application of the boundary conditions and combination of these equations to eliminate $\bar{\theta}_s$ gives:

$$\bar{\theta}_t = \frac{K_{ti}K_{si}}{V_{ti}V_{si}}\,e^{-\alpha_2 x}\int_0^x e^{(\alpha_1+\alpha_2)x}\,dx\int_x^L e^{-\alpha_1 x}\,\bar{\theta}_t dx$$

$$+\frac{K_{ti}}{V_{ti}}N_1 e^{-\alpha_2 x}\int_0^x e^{(\alpha_1+\alpha_2)x}\,dx\int_x^L e^{(m_2-\alpha_1)x}\,\bar{V}_s dx$$

$$-N_2 e^{-\alpha_2 x}\int_0^x e^{(m_2+\alpha_2)x}\,\bar{V}_t dx \qquad \text{(Eq. 8)}$$

Define the integral operator $I(\bar{\theta}_t)$ as

$$I(\bar{\theta}_t) = \frac{K_{ti}K_{si}}{V_{ti}V_{si}}\,e^{-\alpha_2 x}\int_0^x e^{(\alpha_1+\alpha_2)x}\,dx\int_x^L e^{-\alpha_1 x}\,\bar{\theta}_t dx$$

Let the function f(x, s) be

$$f(x,s) = \frac{K_{ti}N_1}{V_{ti}} e^{-\alpha_2 x} \int_0^x e^{(\alpha_1 + \alpha_2)x} dx \int_x^L e^{(m_2 - \alpha_1)x} \overline{V}_1 dx$$

$$- N_2 e^{-\alpha_2 x} \int_0^x e^{(m_2 + \alpha_2)x} \overline{V}_2 dx$$

Equation 6 may now be written as

$$\overline{\theta}_t = I(\overline{\theta}_t) + f(x,s)$$

Solving for $\overline{\theta}_t$ gives the following result for $I < 1$

$$\overline{\theta}_t = \frac{f(x,s)}{1 - I} \qquad \text{(Eq. 9)}$$

The right side of Equation 9 may be expanded in a series to give:

$$\overline{\theta}_t = \sum_{n=0}^{\infty} I^n\{f(x,s)\}$$

where I^n means that the operation I is applied n times.

For $n = 0$ it is easily seen that $\overline{\theta}_t = f(x,s)$ and therefore the double integral of $\overline{\theta}_t$ is neglected in the one term approximation. Going back to the origin of Equation 8, it may be seen that this double integral term represents the change in $\overline{\theta}_t$ caused by the interaction between $\overline{\theta}_t$ and $\overline{\theta}_s$

when an upset occurs. For instance an upset in V_t causes a change in θ_t which then causes θ_s to change. The change in θ_s then reflects back to the tube causing another small change in θ_t. This is the effect that is neglected in the one term approximation of $\overline{\theta}_t/\overline{V}_t$ which yields Model IV given previously. Consideration of higher order terms in the series will account for the effect of higher order temperature reflections between the shell and tube.

For an upset in V_s, a change in θ_s results which causes a corresponding change in θ_t. This change in θ_t reflects back to the shell causing further change in θ_s which then causes more change in θ_t. It is this latter temperature reflection that is neglected in the first term approximation of $\overline{\theta}_t/\overline{V}_s$ which is as follows:

$$\frac{\overline{\theta}_{tL}}{\overline{V}_s} = \frac{K_{ti}N_1 e^{m_2 L}}{V_{ti}(m_2 - \alpha_1)(\alpha_1 + \alpha_2)}\left(1 - e^{-(\alpha_1 + \alpha_2)L}\right)$$

$$- \frac{K_{ti}N_1}{V_{ti}(m_2 - \alpha_1)(m_2 + \alpha_2)}\left(e^{m_2 L} - e^{-\alpha_2 L}\right) \qquad \text{Model V}$$

The second term of the series approximation of $\overline{\theta}_t/\overline{V}_t$ was also developed and compared with experimental data, but it is complex and was found to have very small effect upon frequency response results so it is not given here.

Transient response

To use the partial differential equation transfer function Models I through V to predict transient response, it is necessary to invert the equations to real time and solve for θ_{tL} by substituting different values of time into the equation. However, it is known that the final temperature predicted is very strongly dependent upon heat transfer coefficient variation with flow changes, so only Models I and III which account for the effect of heat transfer coefficient variation can be expected to predict accurate transient response curves.

Inverting Model III yields:

$$\theta_{tL} = \frac{-V_t'(N_2 + R_2)V_{ti}e^{m_2 L}}{K_{ti} + m_2 V_{ti}} \left\{1 - e^{-(K_{ti} + m_2 V_{ti})t}\right\}$$

$$- \frac{V_t' Q_2}{K_{ti}} \left(1 - e^{-K_{ti} t}\right)$$

$$+ \mathcal{U}(t - L/V_{ti}) \left[\frac{V_t'(N_2 + R_2)V_{ti}e^{-LK_{ti}/V_{ti}}}{K_{ti} + m_2 V_{ti}}\right.$$

$$\left\{1 - e^{-(K_{ti} + m_2 V_{ti})(t - L/V_{ti})}\right\}$$

$$\left. + \frac{V_t' Q_2 e^{-LK_{ti}/V_{ti}}}{K_{ti}} \left\{1 - e^{-K_{ti}(t - L/V_{ti})}\right\}\right] \qquad \text{Model VI}$$

where $\mathcal{U}(t - L/V_{ti})$ is the unit function.

Model VI predicts reasonably good transient response results for small flow upsets but gives poor results for large flow upsets. This apparently is due to the dropping of terms involving products of perturbations when Equations 4 and 5 are reduced to constant coefficient equations. For instance, when a flow rate is increased from one to two feet per second the perturbation is as large as the initial steady state flow rate and dropping the product of this perturbation and a resulting temperature perturbation introduces a very significant error into the final temperature predicted. For small perturbations relative to a steady state flow rate, the steady state terms are large compared to the perturbation terms so dropping the terms involving products of perturbations does not introduce significant error into the equations. Frequency response results are not as readily effected by large flow upsets because normalized frequency response data do not depend upon the magnitude of the upset. Since frequency response amplitude ratios are obtained by dividing the temperature response amplitude at any frequency by the steady state amplitude at $\omega = 0$, the effect of perturbation magnitude is eliminated in one term models such as Model IV. The effect of perturbation magnitude is also very small when more than one term appears in a model, such as Models III and V, because the terms vary

proportionally with the upset magnitude.

Lumped Parameter Models

Another way of approximating the unsteady state temperature response of shell and tube fluids is by representing the distributed parameter system with a lumped parameter model, i.e., a model that is a function of time only rather than both time and distance. This can be accomplished by assuming that the temperature variation in both the shell and tube is linear with respect to x. This gives the following definitions:

$$\frac{\partial \theta_s}{\partial x} = \frac{\theta_{sL} - \theta_{s0}}{L}, \qquad \frac{\partial \theta_t}{\partial x} = \frac{\theta_{tL} - \theta_{t0}}{L}$$

Applying these definitions to Equations 4 and 5 and assuming arithmetic average temperature driving forces in the terms on the right side of Equations 4 and 5 yields the following ordinary differential equations after the steady state equations have been subtracted from the total equations:

$$\frac{d\theta'_{tL}}{dt} + \left(\frac{V_t}{L} + \frac{K_t}{2}\right)\theta'_{tL} = -\frac{(\theta_{tLi} - \theta_{t0i})}{L} V'_t + \frac{K_t}{2}\theta'_{s0}$$

$$+ \frac{(\theta_{sLi} + \theta_{sOi} - \theta_{tLi} - \theta_{tLi})}{2} K_t'$$

$$\frac{d\theta_{sO}'}{dt} + (\frac{V_s}{L} + \frac{K_s}{2})\theta_{sO}' = \frac{(\theta_{sLi} - \theta_{sOi})}{L} V_s' + \frac{K_s}{2} \theta_{tL}'$$

$$+ \frac{(\theta_{tLi} + \theta_{tOi} - \theta_{sLi} - \theta_{sOi})}{2} K_s'$$

Model VII

where variables are represented as the sum of perturbations plus steady state terms as previously defined.

$$V_t = V_{ti} + V_t', \qquad V_s = V_{si} + V_s', \qquad K_s = K_{si} + K_s',$$

$$K_t = K_{ti} + K_t', \qquad \theta_{tL} = \theta_{tLi} + \theta_{tL}', \qquad \theta_{sO} = \theta_{sOi} + \theta_{sO}'$$

Note that the products of perturbations have not been dropped. Model VII can be solved quickly on an analog computer to obtain the output temperature response of the shell or tube fluid forced by transient or frequency upsets in either flow rate or simultaneous upsets of both flow rates. Mean values of V_t, V_s, K_t, K_s are used for frequency response, whereas the new values after an upset are used for transient response. To predict frequency response results for upsetting one flow rate it was found convenient to

reduce Model VII to transfer function form and solve by letting $s = i\omega$. To accomplish this it is necessary to let

$$K_s' = K_{si}\left(k_s \frac{V_s'}{V_{si}} + k_t \frac{V_t'}{V_{ti}}\right) \text{ and } K_t' = K_{ti}\left(k_s \frac{V_s'}{V_{si}} + k_t \frac{V_t'}{V_{si}}\right).$$

Combining the two equations in Model VII to eliminate θ_{sO}' and transforming the resulting equation with respect to time yields the following transfer functions.

For convenience let $E = \theta_{tLi} + \theta_{tOi} - \theta_{sLi} - \theta_{sOi}$

$$\frac{\overline{\theta}_{tL}}{\overline{V}_t} = -\frac{-\dfrac{EK_tK_{si}k_t}{4V_{si}} + \left(\dfrac{EK_{ti}k_t}{2V_{ti}} + \dfrac{\theta_{tLi} - \theta_{tOi}}{L}\right)s + \left(\dfrac{V_s}{L} + \dfrac{K_s}{2}\right)\left(\dfrac{EK_{ti}k_t}{2V_{ti}} + \dfrac{\theta_{tLi} - \theta_{tOi}}{L}\right)}{s^2 + \left(\dfrac{V_t + V_s}{L} + \dfrac{K_t + K_s}{2}\right)s + \dfrac{V_tV_s}{L^2} + \dfrac{K_tV_s + K_sV_t}{2L}}$$

Model VIII

$$\frac{\overline{\theta}_{tL}}{\overline{V}_s} = \frac{\dfrac{(\theta_{sLi} - \theta_{sOi})K_t}{2L} + \dfrac{EK_{si}K_tk_s}{4V_{si}} - \left(\dfrac{V_s}{L} + \dfrac{K_s}{2}\right)\dfrac{EK_{ti}k_s}{2V_{si}} - \dfrac{EK_{ti}k_s}{2V_{si}}s}{s^2 + \left(\dfrac{V_t + V_s}{L} + \dfrac{K_t + K_s}{2}\right)s + \dfrac{V_tV_s}{L^2} + \dfrac{K_tV_s + K_sV_t}{2L}}$$

Model IX

EXPERIMENTAL INVESTIGATION

Equipment and Materials

A double pipe heat exchanger was constructed that could be operated as a co-current, counter-current or steam-water heat exchange system with only minor changes in the piping system. A flow sheet of the counter-current system used in this investigation is shown in Figure 1. The heat exchanger was constructed with a 1 inch nominal type K copper tube concentrically mounted inside a 2 inch nominal schedule 40 iron pipe shell. The exchanger was 14.7 feet long from the center line of the shell input to center line of the shell output. The shell was insulated with 3/4 inch Fiberglass pipe insulation. Hot water flowed through the tube from the constant head tank and was cooled by counter-current cold water from the university water line flowing in the shell. Steam injected into water flowing into the constant head tank produced the hot water. The flows of input water and steam were regulated to obtain a desired water temperature. The heated water was discharged into an elevated 55 gallon hold-up tank at a flow rate great enough to always maintain an overflow. This provided a constant temperature and constant pressure hot water source.

A series thermocouple with seven probes constructed of

Figure 1. Flow diagram of counter-current heat exchange system

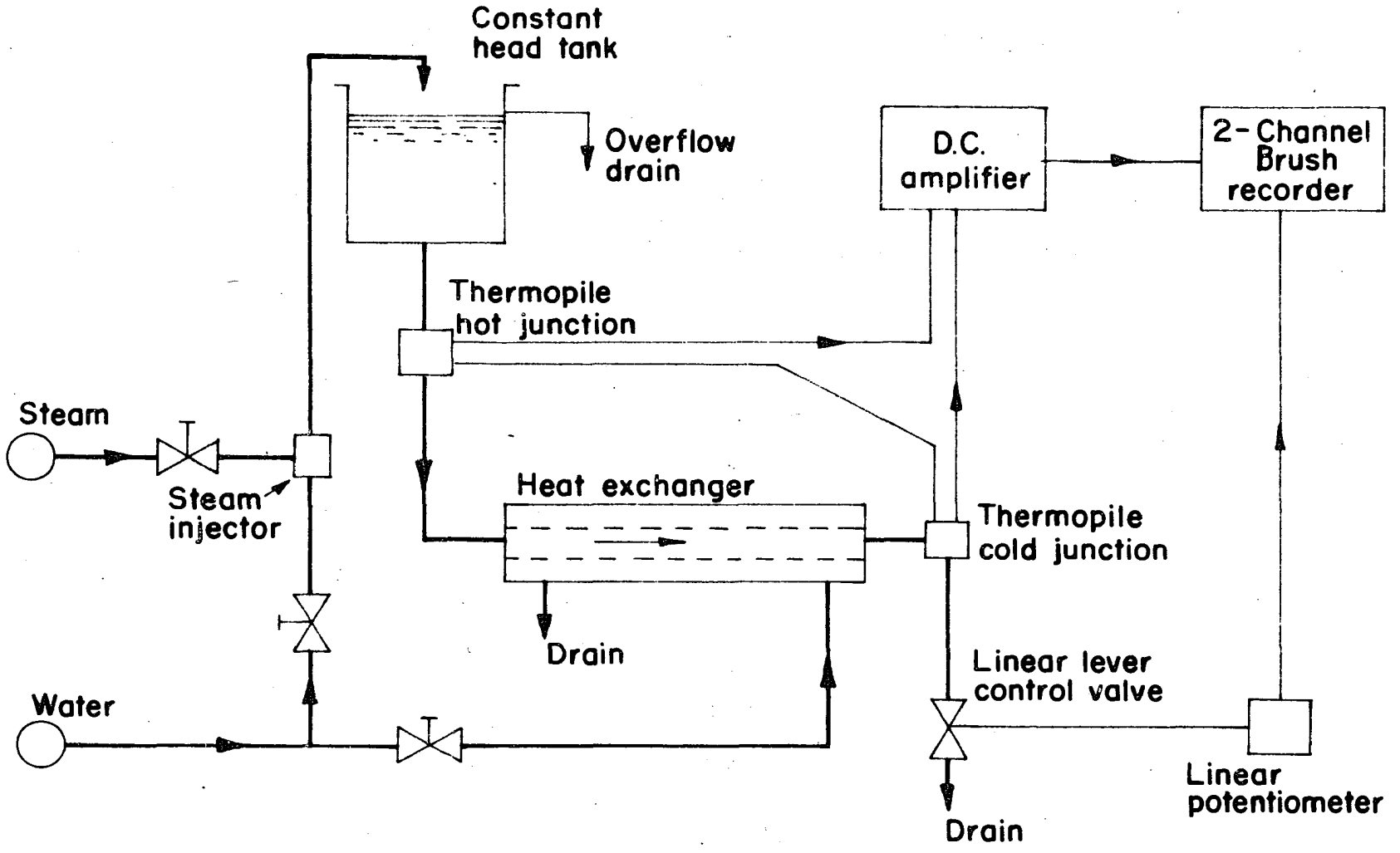
Constant
head tank
Overflow
drain
D.C.
amplifier
2-Channel
Brush
recorder
Thermopile
hot junction
Steam
Steam
injector
Heat exchanger
Thermopile
cold junction
Drain
Linear lever
control valve
Water
Linear
potentiometer
Drain

24 gauge copper-constantan wire was placed in the outlet tube stream to provide a continuous temperature signal to D.C. amplifier-recorder equipment. The time constant of the thermopile for temperature changes of 100° F is less than one-tenth of a second. The thermopile was mounted in a long probe so that it could be inserted into the end of the heat exchanger such that measurement of the temperature of tube fluid at the center line of entering shell fluid could be effected. This eliminated temperature measurement transport lag. The measuring junction of the thermopile was the cold junction of the couple because the hot junction was placed in a constant temperature bath of the hot fluid flowing from the constant head tank. Thus, the thermopile signal always indicated the temperature difference between input and output fluid in the tube.

Steady state measurement of input and output shell and tube temperatures was accomplished with mercury-in-glass thermometers placed in thermowells in the appropriate lines. Steady state flow rates were measured by collecting the effluent streams for a known length of time and weighing the amount on a platform scale. For frequency analysis the maximum and minimum flow rates were measured at the start of a run and variation of flow rate with valve position was assumed to be linear between these limiting flow rates. Calibration of the valves controlling both the shell and

tube flow rates showed this to be a good assumption for the flow ranges studied in this investigation. The valve used to control the varying tube flow rate was a 3/4 inch Fisher lever valve with 5/8 inch stem travel installed in the tube outlet water line. A similar valve was installed in the shell water line to permit the study of shell flow rate upsets.

A mechanical sine generator was used to actuate the lever valve for frequency analysis experiments. The mechanism consisted of a 1/8 horsepower motor driving two Zeromax Variable Speed drives coupled in series. The second Zeromax speed reducer drove a cam arrangement which produced the sine wave. Frequencies were varied by means of the variable speed drives with a frequency range from zero to one cycle per second.

Continuous recording of changes in flow rate was made possible by using a Bourn linear sliding arm potentiometer in series with a $1\frac{1}{2}$ volt D.C. battery. The sliding arm of the potentiometer was spring loaded against the lever of the flow control valve and thus continuously converted the valve position into an electrical signal which was recorded on one channel of a two channel strip-chart Brush Recorder. Temperature response from the thermopile signal was recorded on the second Brush Recorder channel after the thermopile signal had been amplified by a high gain D.C. amplifier. This

simultaneous side by side recording of the input flow forcing signal and the output temperature response signal made it very convenient to obtain magnitude ratio and phase lag information from frequency response data. Catheron and Hainsworth (2) showed that water has no capacity for the storage of flow energy at frequencies below 60 cycles per second, so measuring valve position gives flow rate variation directly.

Procedure and Results

To start a run, the water and steam valves were opened and adjusted to give the desired temperatures and flow rates. The sine generator was positioned to give approximately the desired amplitude of flow variation. Flow rates were then measured and adjusted to exact desired values. About one hour was then allowed for the system to reach steady state. When it was evident that the temperatures had reached their steady state values, frequency response data were taken. Frequency response data were obtained by injecting a sinusoidal flow disturbance into the exchanger and comparing the response and input sinusoids at steady state conditions on the basis of magnitude ratio and phase shift. This was done by first pulsing the water flow rate at a very low frequency of about 0.10 cycle per minute, recording data for

two or three cycles, then increasing the pulse frequency by a small amount and repeating the process. In this manner the desired frequency range covering frequencies up to about 15 cycles per minute was covered in a series of about fifteen steps. At higher frequencies more cycles were observed to insure that steady state frequency response conditions were attained. Inlet temperatures were checked periodically to insure that the initial conditions of a run were not changing. If any of these readings showed a change of more than one degree, the run was repeated.

Six tests were made at various flow conditions as shown in Table 1. Each test consisted of taking both transient and frequency response data over the same flow range. Resonance was observed for each of the six frequency response tests and was found to be a function only of heat exchanger length (L), upset frequency of either fluid (ω), and velocity of the fluid (V) whose temperature was being measured (not necessarily the fluid being upset). For all tests, resonance occurred when $L\omega/V = 2\pi$, where the resonance frequency is defined as the frequency at which the amplitude ratio ceases to attenuate and starts to get larger. Tests 1 and 2 with unequal mass flow rates in the shell and tube were made to see if any difference could be observed between frequency response results for large and small tube flow changes about the same mean flow rate. Tests 1 and 2 had

Table 1. Steady state data for the maximum and minimum flow rates of six counter-current experimental frequency and transient response tests

	W	θ_{sOi}	θ_{sLi}	θ_{tOi}	θ_{tLi}	U
	lb/min	(^{o}F)	(^{o}F)	(^{o}F)	(^{o}F)	BTU/min ft^{2} ^{o}F
Test 1 (tube upset)						
Wmax	35.0	66.2	59.0	153.5	110.0	5.85
Wmin	21.5	64.2	59.0	153.5	102.5	4.46
Wshell	210					
Test 2 (tube upset)						
Wmax	31.0	65.7	59.0	153.5	108.0	5.50
Wmin	25.5	64.9	59.0	153.5	105.0	4.95
Wshell	210					
Test 3 (tube upset)						
Wmax	30.5	87.0	59.0	152.0	131.0	2.42
Wmin	15.5	81.0	59.0	152.0	120.5	1.94
Wshell	23.0					

Table 1. (Continued)

	W lb/min	θ_{sOi} (^{o}F)	θ_{sLi} (^{o}F)	θ_{tOi} (^{o}F)	θ_{tLi} (^{o}F)	U BTU/min ft^2 ^{o}F
Test 4 (tube upset)						
Wmax	26.0	85.0	59.0	152.0	129.0	2.27
Wmin	20.0	83.0	59.0	152.0	124.5	2.10
Wshell	23.0					
Test 5 (shell upset)						
Wmax	66.0	75.0	59.0	164.0	125.5	3.44
Wmin	27.0	85.7	59.0	164.0	136.0	2.42
Wtube	26.0					
Test 6 (simultaneous shell and tube upset)						
$W_s$max	55.0	68.5	48.5	158.0	128.0	3.24
$W_t$max	34.0	68.5	48.5	158.0	128.0	3.24
$W_s$min	30.0	72.0	48.5	158.0	124.0	2.30
$W_t$min	21.0	72.0	48.5	158.0	124.0	2.30

respective tube flow upsets of 65 per cent and 26 per cent of a 23.0 lb/min mean flow rate. Tests 3 and 4 had respective tube flow upsets of 48 per cent and 21 per cent of a 28.2 lb/min mean tube flow rate. Shell flow rate was equal to 210 lb/min for Tests 1 and 2, but was equal to mean tube flow for Tests 3 and 4. The large flow changes did not give frequency response results significantly different from the small flow changes as may be seen in Figures 2 and 3. Transient response data were measured over the same flow ranges that frequency response data were taken for Tests 1 to 4. These transient response curves for both increases and decreases in flow rate are plotted in Figures 8 to 11. The response curves may be seen to exhibit the mild second order effect of initially having a slope of zero.

Test 5 was conducted for shell flow upsets forcing output tube temperature to see if shell flow upsets gave any notable differences in the frequency and transient response curves from the tube flow upsets of Tests 1 to 4. Frequency response data of Test 5 are plotted in Figure 6 and are generally similar to the tube flow upset data. The resonance frequency was found to be a function only of the tube flow rate, and the frequency at which resonance occurs is readily predictable using $L\omega/V = 2\pi$ where V is the velocity of tube flow rate. Shell temperature response resonance would be at a much different frequency than the tube resonance because

average shell flow is almost twice the tube flow. This would cause shell resonance to occur at a frequency almost twice as great as the tube resonance frequency.

Transient results for Test 5 presented in Figure 12 showed a more pronounced second order effect than the tube flow results of Tests 1 to 4. This was expected since dynamics of both the shell and tube are of equal importance in this case. It may be noted that shell flow increases cause the shell temperature to be cooler which results in a decreasing tube temperature, whereas a tube flow increase causes hot tube fluid to increase in temperature.

Test 6 consisted of pulsing both the shell and tube flow rates sinusoidally with output tube temperature response measured. Frequency response results were similar in general to Tests 1 to 5 and are presented in Figure 17. The resonance frequency was again predictable using $L\omega/V = 2\pi$ for the tube fluid flow rate. Transient results are given in Figure 13.

Phase lag information was obtained from the strip charts by comparing the positions of the peaks of the valve position curve and the outlet water temperature curve. The distance between a response peak and the valve position peak was expressed as degrees of lag based on 360 degrees per cycle. The phase lags plotted in all frequency response curves are average values of the phase lags for the maximum and minimum

flow rates because the phase lags at maximum and minimum flow are different due to the variation in the system time constant with flow changes.

Magnitude ratio information was obtained from the strip charts in the following manner: At very low frequencies the maximum and minimum temperatures of the outlet water equal the steady state temperatures for the corresponding maximum and minimum flow rates. The amplitude ratio, which is equal to response amplitude divided by input amplitude, was considered to be 1.00 at zero frequency. The amplitude of the response at zero frequency was divided into the amplitudes at other frequencies to obtain magnitude ratios less than one at any given frequency greater than zero.

Transient increases in tube flow gave considerably different tube temperature response curves than transient decreases in flow rate over the same flow range. This difference occurs because flow rate and overall heat transfer coefficient both directly affect the time constant of the system. Flow rate upsets change the residence time of tube fluid and this effect is predominant for tube flow upsets. The curves for transient increases and decreases in shell flow are very similar, which further points out the dominance of the residence time in controlling system dynamics. For shell flow upsets forcing tube fluid temperature the tube fluid residence time does not change, so the dynamic

response is nearly the same for both increases and decreases in flow. This emphasized the importance of the length/velocity ratio which gives residence time in distributed parameter system dynamics.

DISCUSSION OF EXPERIMENTAL AND THEORETICAL RESULTS

The frequency response results for Tests 1 through 6 show that resonance is a very dominant factor in determining the shape of frequency response curves for this system. The term resonance is used here to mean the increase of amplitude ratio with increasing upset frequency. Resonance frequency refers to the frequency at which the amplitude ratio ceases to attenuate and starts to get larger with increasing frequency.

Resonance occurs in distributed parameter processes and does so because of variation in the length of time an element of fluid takes to pass through the tube of a heat exchanger. For two fluid flow, each fluid has its own independent resonance frequency. For illustrative purposes consider a constant shell temperature tube flow upset forcing tube temperature. At steady state all elements of tube fluid have the same residence time in the exchanger. When flow rate is pulsed sinusoidally at low frequencies, some elements of fluid enter the exchanger at maximum flow and require less time to pass through the exchanger than those that enter at minimum flow. Thus, some elements of fluid are heated more than others and a periodic temperature response curve results. As upset frequency is increased the response curve attenuates because the average residence time an element of

fluid that entered the exchanger at maximum flow rate becomes smaller and the residence time becomes larger for the fluid element entering at minimum flow rate. The resonance frequency occurs when the upset frequency in cycles per minute equals the reciprocal of the residence time in minutes of an element of fluid at mean flow rate. At this frequency an inversion takes place in the trend of residence times for fluids that are in the exchanger the maximum or minimum length of time. Increasing the frequency above the resonance frequency causes the maximum residence time element of fluid to be in the exchanger a longer period of time rather than a shorter time, and vice versa for the minimum residence time fluid element. This causes the temperature response amplitude to get larger rather than attenuate. Increasing the upset frequency further causes attenuation again for similar reasons. At the resonance frequency each element of fluid requires the same length of time to pass through the heat exchanger, regardless of whether it enters the exchanger at maximum, minimum or average flow. Each element passes through one full sinusoidal flow cycle as it traverses the exchanger, so the average residence times are all equal to the mean flow residence time. Therefore, for tube flow upsets forcing tube temperature at the resonance frequency, the temperature response curve would be a straight line (zero amplitude ratio) if a perfect sinusoidal flow upset

was being impressed upon the system and if the variations in temperature driving forces along the length of the heat exchanger were a negligible consideration. For steam temperature or shell flow upsets forcing tube fluid temperature at the resonance frequency, a straight line temperature response would not be expected because the variation in temperature driving force along the heat exchanger length is an important consideration. For example, for steam temperature upsets forcing the temperature of tube fluid with a constant flow rate a different amount of heat transfer would take place if maximum temperature steam initially contacted the inlet cold tube fluid than if low temperature steam initially contacted the fluid. The average steam temperature in contact with all elements of fluid traversing the exchanger would be the same, but the heat transfer attained would be expected to differ because of driving force variation.

The frequency response results for tube, shell and simultaneous tube and shell flow upsets verify that resonance depends upon the L/V ratio of the fluid whose temperature is being measured and that, in fact, resonance occurs when $L\omega/V = 2\pi$ with ω expressed in radians per second. This is also predicted theoretically with any of the appropriate partial differential equation Models I to V. Wall capacitance and heat transfer coefficient variation do not affect the resonance frequency. In each of Models I to V, the

transport delay term $e^{-iL\omega/V}$ appears. This may be expanded to equal cos $L\omega/V$ - i sin $L\omega/V$. The sine and cosine terms repeat themselves at every multiple of 2π which is the factor which causes resonance to be predicted when $L\omega/V = 2\pi$ or integral multiples of 2π. The same transport term exists in the models for steam temperature upsets previously presented (23). If the temperature reflections or higher order terms in the series approximation solution are considered, transport delay terms appear that would predict resonance at a different frequency, but these terms are always small compared to the $e^{-iL\omega/V}$ transport term and the latter term dominates.

In Figures 2 and 3 it may be observed that the magnitude of flow rate perturbations had no significant effect on frequency response results in the range of flow upsets studied and that Model IV, which was developed from partial differential equations neglecting wall capacitance and heat transfer coefficients variation, gives good agreement with experimental data. Theoretical frequency response results do not depend upon the upset magnitude because normalizing the amplitude ratios eliminates the effect of perturbation size. The fact that Model IV gives good theoretical agreement with experimental tests for equal shell and tube flow rates as well as the large shell flow rate tests with nearly constant shell temperature is important. This verifies the

Figure 2. Experimental frequency response for Tests 1 and 2 and theoretical frequency response obtained using Model IV

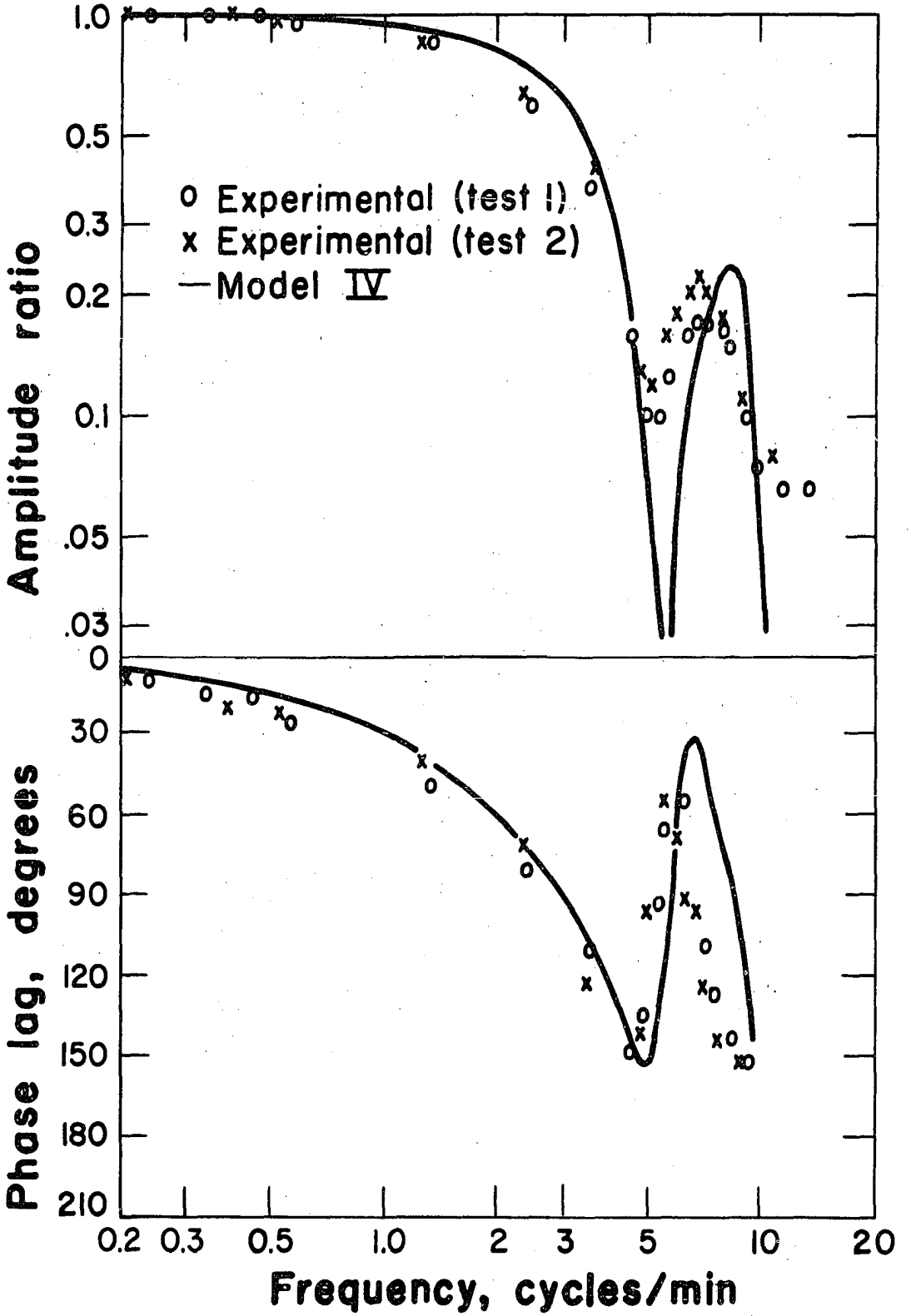
o Experimental (test 1)
x Experimental (test 2)
—Model IV
Amplitude ratio
1.0
0.5
0.3
0.2
0.1
.05
.03
0
Phase lag, degrees
30
60
90
120
150
180
210
0.2
0.3
0.5
1.0
2
3
5
10
20
Frequency, cycles/min

Figure 3. Experimental frequency response for Tests 3 and 4 and theoretical frequency response obtained using Model IV

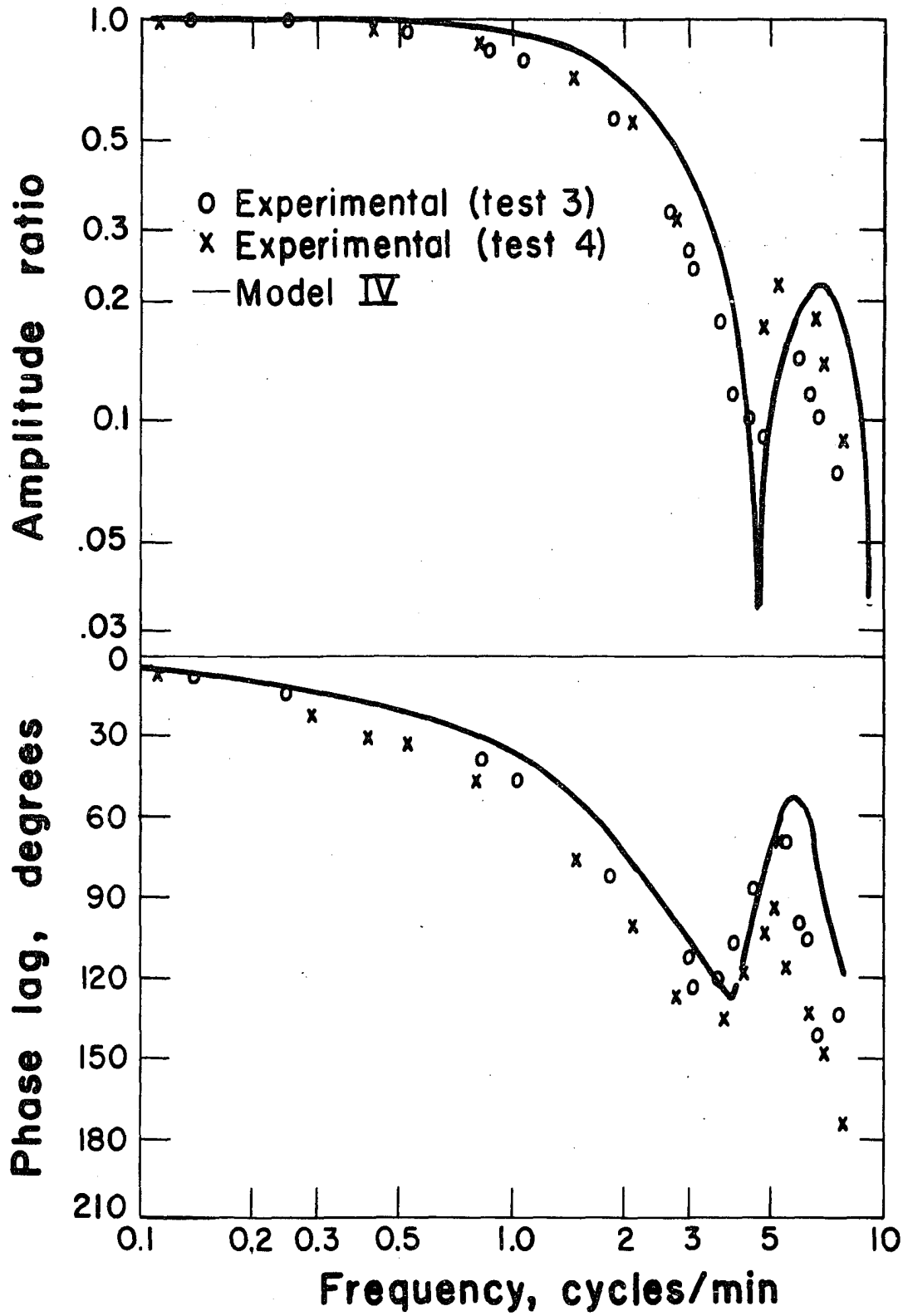
Amplitude ratio
1.0
0.5
0.3
0.2
0.1
.05
.03
o Experimental (test 3)
x Experimental (test 4)
—Model IV
Phase lag, degrees
0
30
60
90
120
150
180
210
0.1
0.2
0.3
0.5
1.0
2
3
5
10
Frequency, cycles/min

validity of neglecting the temperature forcing terms in the derivation of the partial differential equation models.

In Figures 4 and 5 the data of Test 1 and Test 3 were checked with Models I and II to observe the effect of wall capacitance and heat transfer coefficient variation. Figure 4 shows that for Test 1 with a large shell flow, identical theoretical results are obtained with Model I which includes heat transfer film coefficient variation and with Model II which neglects it. These theoretical results are in turn nearly identical with the results of Model IV. This indicates that for a nearly constant shell temperature (high flow rate or steam in shell) heat transfer coefficient variation and wall capacitance are negligible effects. Figure 5 shows that for equal flow rates in the shell and tube a slight improvement resulted by including the heat transfer coefficient variation in Model I. Whether the added work of calculating the extra term in Model I is worth the slight improvement in results is a judgment decision that would have to be based on the accuracy desired.

Comparing the results of Figure 3 and Figure 5 shows that including the effect of wall capacitance softens the resonance frequency dip. Neglecting the heat transfer coefficient variation makes the dip even softer. Including the wall capacitance also gives a slight improvement to phase lag results.

Figure 4. Experimental frequency response for Test 1 and theoretical frequency response obtained using Models I and II

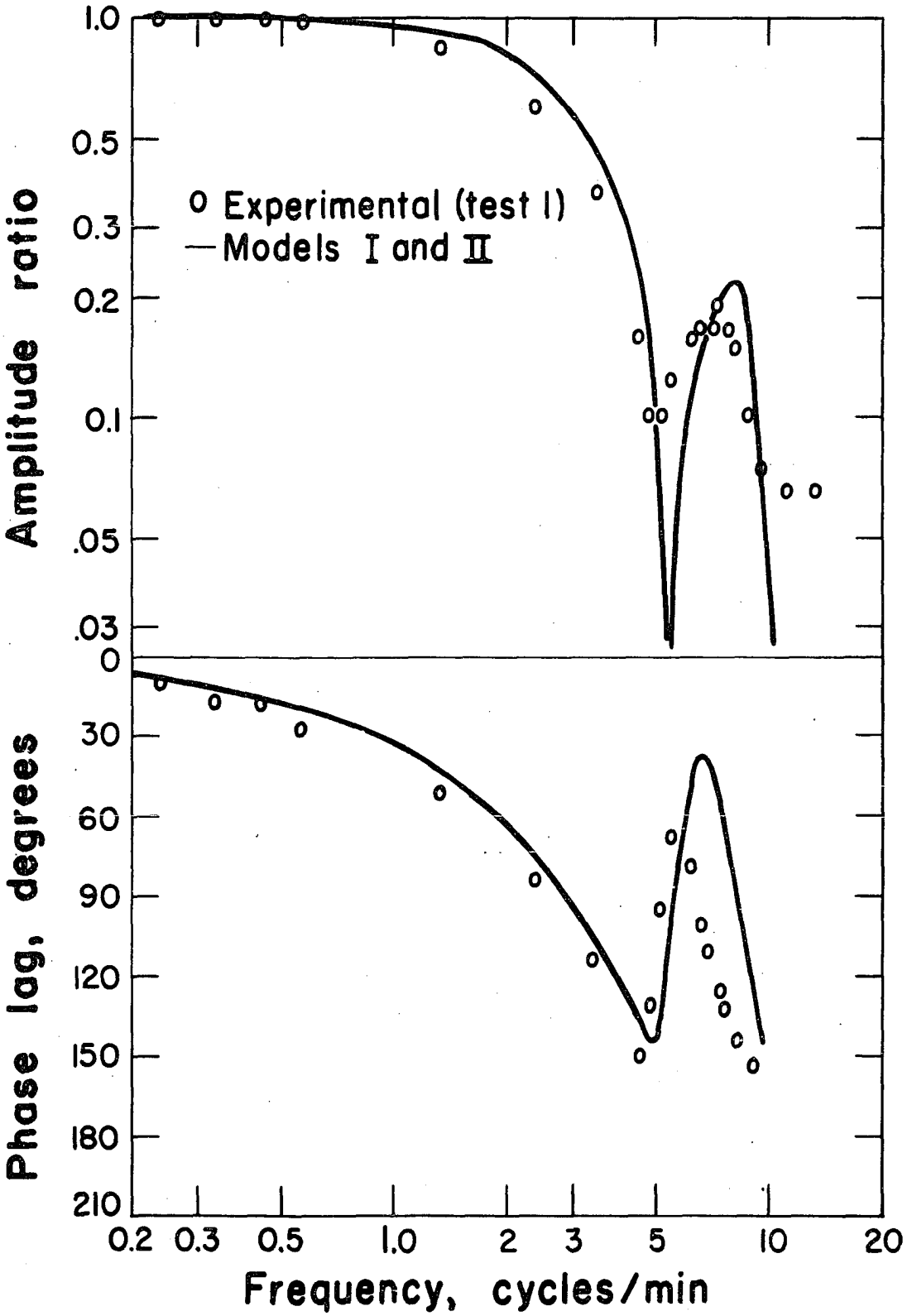
1.0
0.5
0.3
0.2
0.1
.05
.03
Amplitude ratio
o Experimental (test I)
— Models I and II
0
30
60
90
120
150
180
210
Phase lag, degrees
0.2
0.3
0.5
1.0
2
3
5
10
20
Frequency, cycles/min

Figure 5. Experimental frequency response for Test 3 and theoretical frequency response obtained using Models I and II

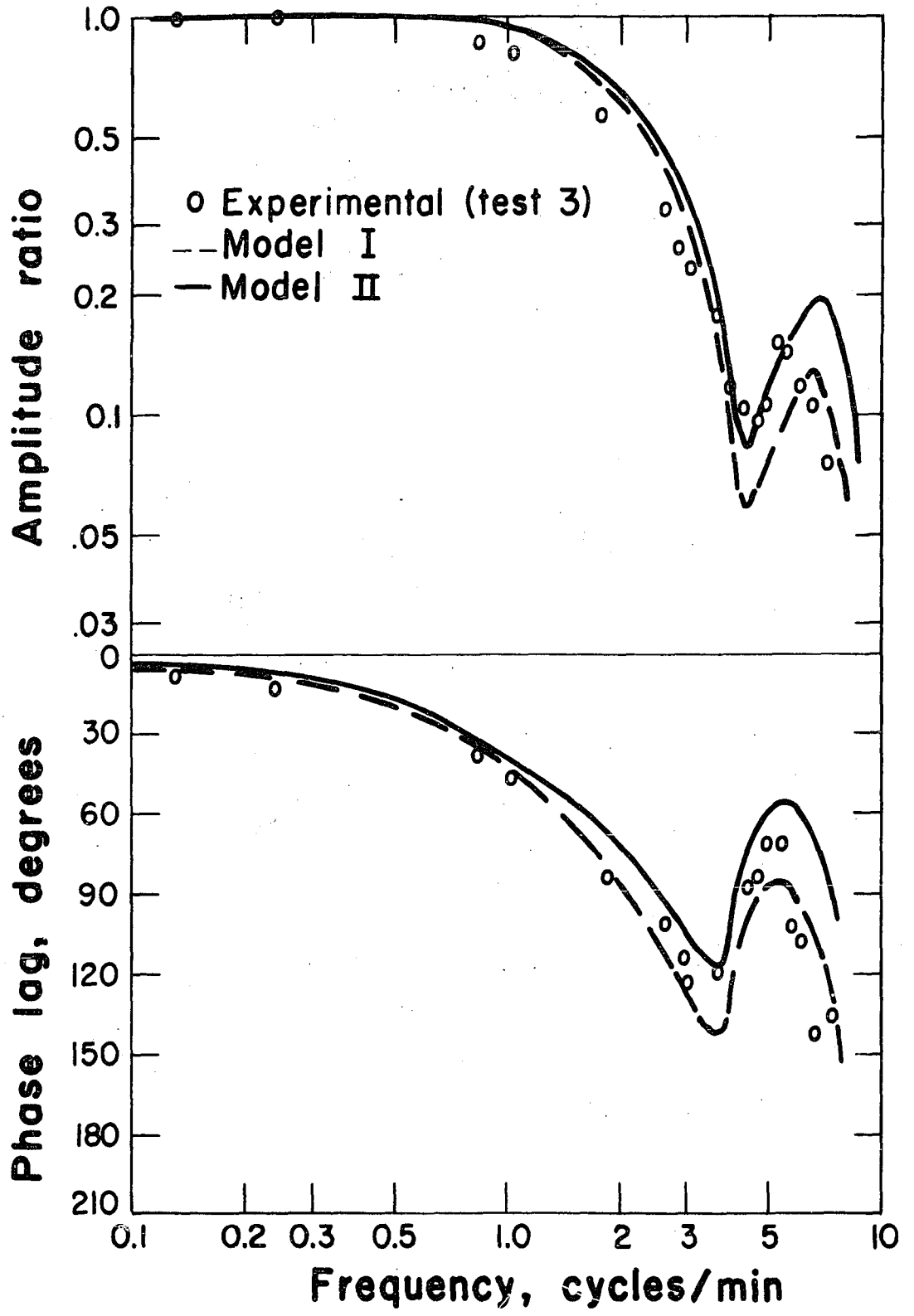
Amplitude ratio
1.0
0.5
0.3
0.2
0.1
.05
.03
o Experimental (test 3)
--Model I
—Model II
Phase lag, degrees
0
30
60
90
120
150
180
210
0.1
0.2
0.3
0.5
1.0
2
3
5
10
Frequency, cycles/min

Figure 6 shows that shell flow upset data of Test 5 are in relatively good agreement with Model V. Phase lag agreement is excellent over the full range of frequencies tested. The resonance frequency dip does not go to zero but is very small.

Transient response data presented in Figure 7 are in fairly good agreement with the predictions of partial differential equation Model VI. Tests 2 and 4 which are presented were for relatively small flow upsets compared to mean flow rates as may be seen in Table 1. Results obtained when Model VI was compared with the transient data of Tests 1 and 3 for large flow upsets were very poor. Final temperatures predicted were in error by 50-75 per cent. This is due to dropping the product of perturbation terms in reducing the partial differential equations to constant coefficient equations. For large upsets the product of perturbation terms may be as large as the steady state terms and neglecting them introduces significant error into final temperatures predicted. Frequency response results are not affected, however, because the effect of perturbation magnitude is eliminated by normalizing the amplitude ratio.

Figures 8 to 13 show that the ordinary differential equation Model VII gives good agreement with experimental transient data for all tests. The theoretical curves do not exhibit the second order effect of having a zero slope

Figure 6. Experimental frequency response for Test 5 and theoretical frequency response obtained using Model V

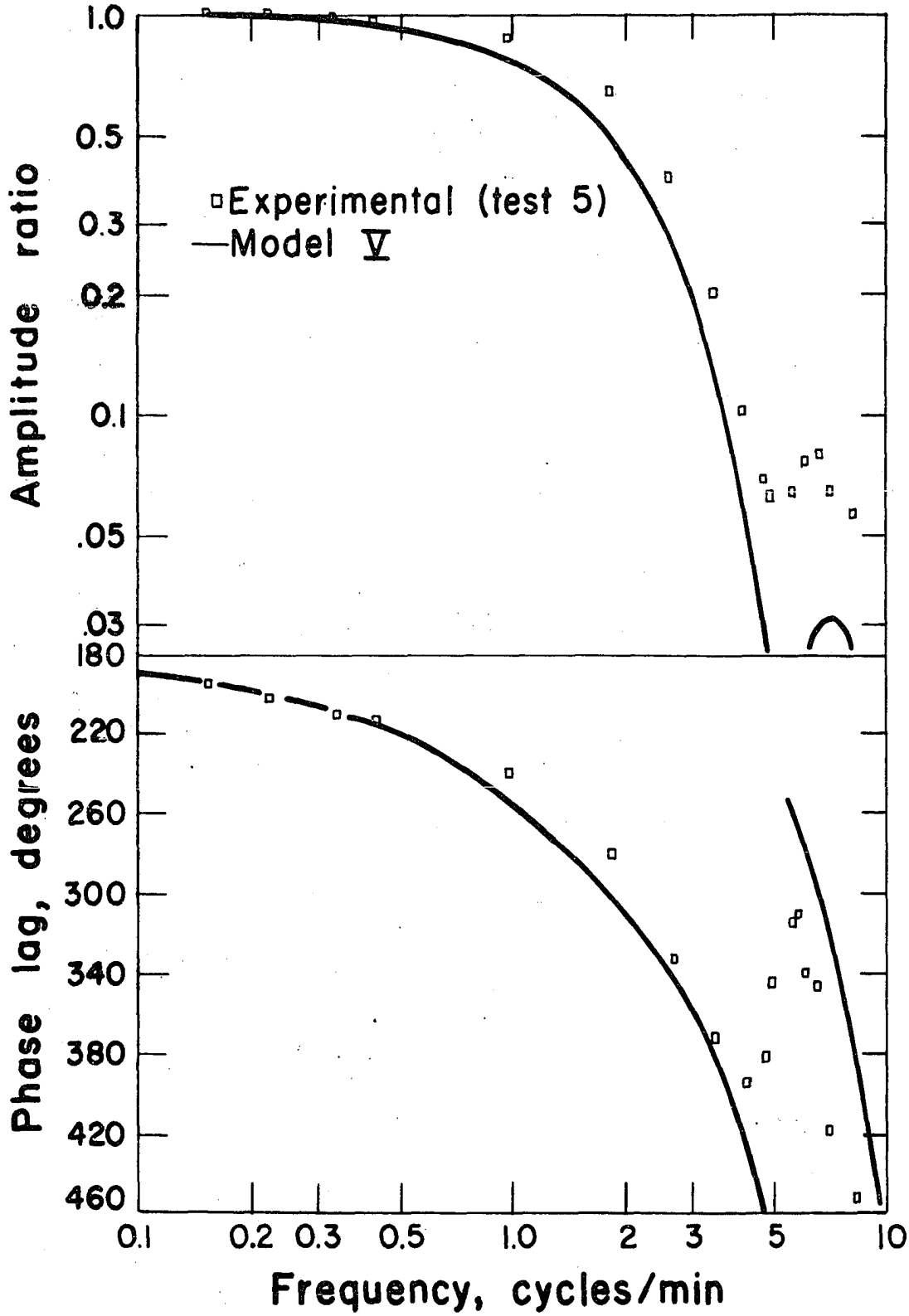
Amplitude ratio
1.0
0.5
0.3
0.2
0.1
.05
.03
Experimental (test 5)
Model V
Phase lag, degrees
180
220
260
300
340
380
420
460
0.1
0.2
0.3
0.5
1.0
2
3
5
10
Frequency, cycles/min

Figure 7. Experimental transient response for Tests 2 and 4 and theoretical transient response obtained using Model VI

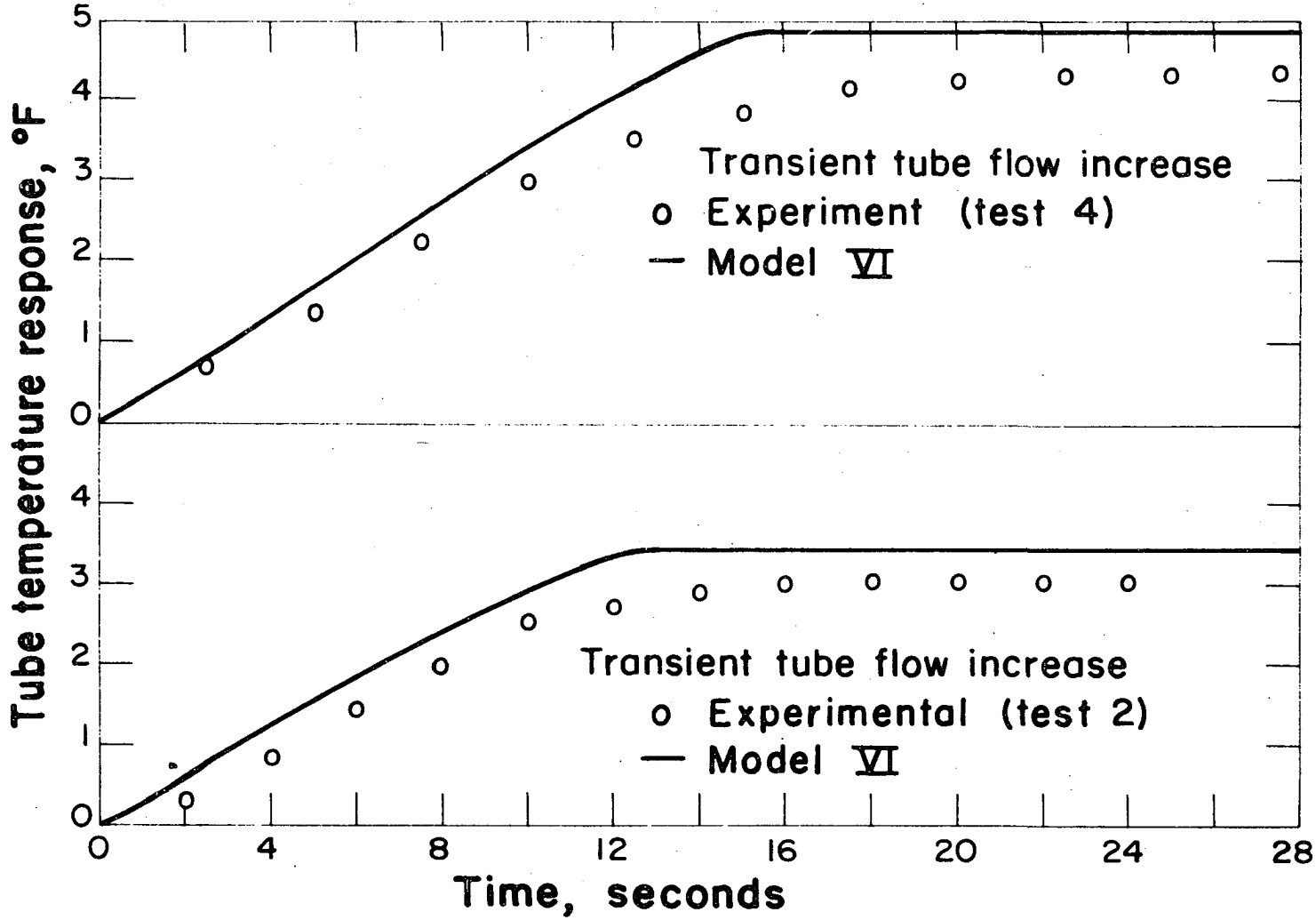
Tube temperature response, °F
Time, seconds
Transient tube flow increase
o Experiment (test 4)
— Model VI
Transient tube flow increase
o Experimental (test 2)
— Model VI
0
1
2
3
4
5
0
4
8
12
16
20
24
28

Figure 8. Experimental transient response for Test 1 and theoretical transient response obtained using Model VII

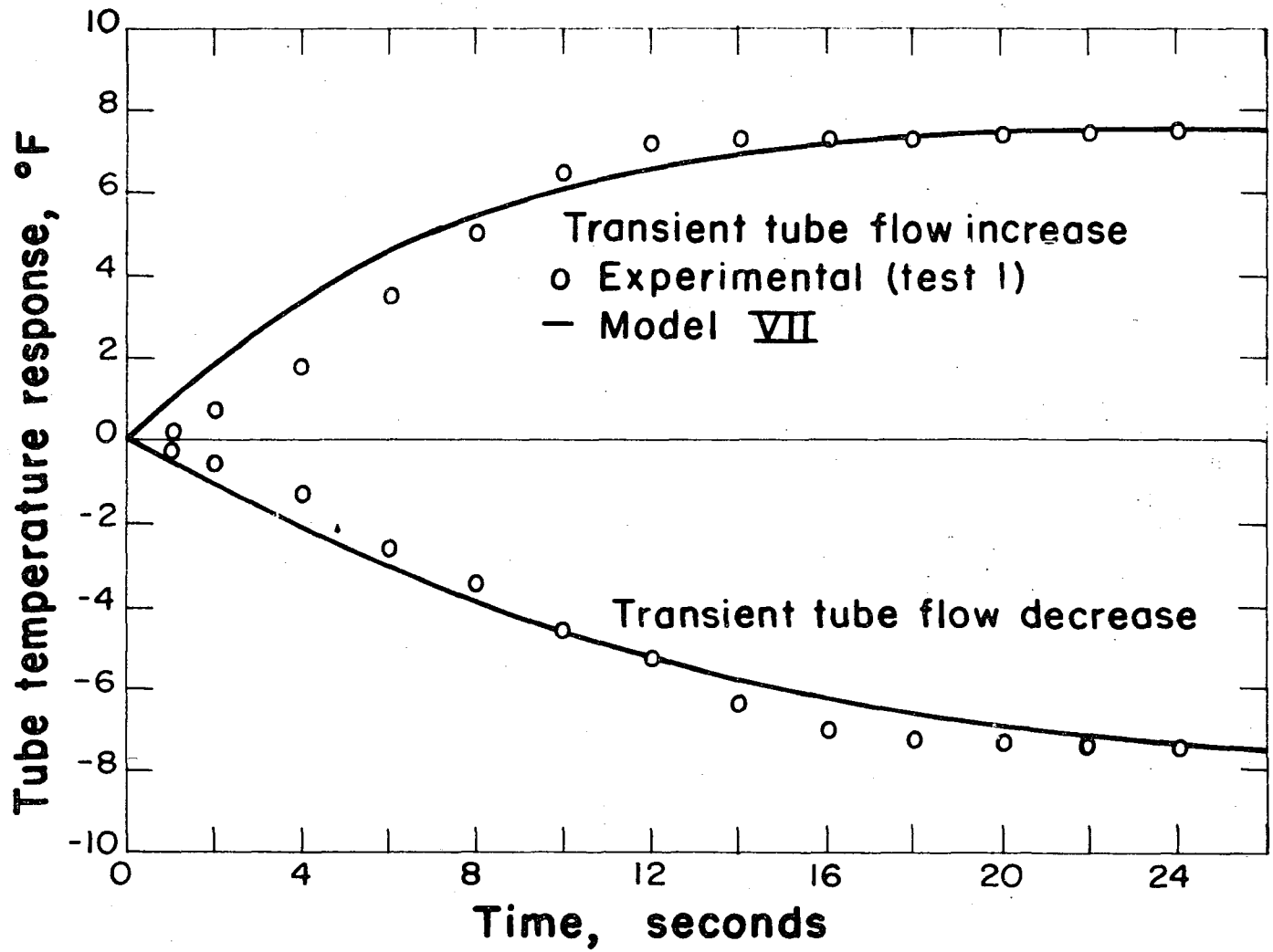
Tube temperature response, °F
10
8
6
4
2
0
-2
-4
-6
-8
-10
0
4
8
12
16
20
24
Time, seconds
Transient tube flow increase
o Experimental (test I)
— Model VII
Transient tube flow decrease

Figure 9. Experimental transient response for Test 2 and theoretical transient response obtained using Model VII

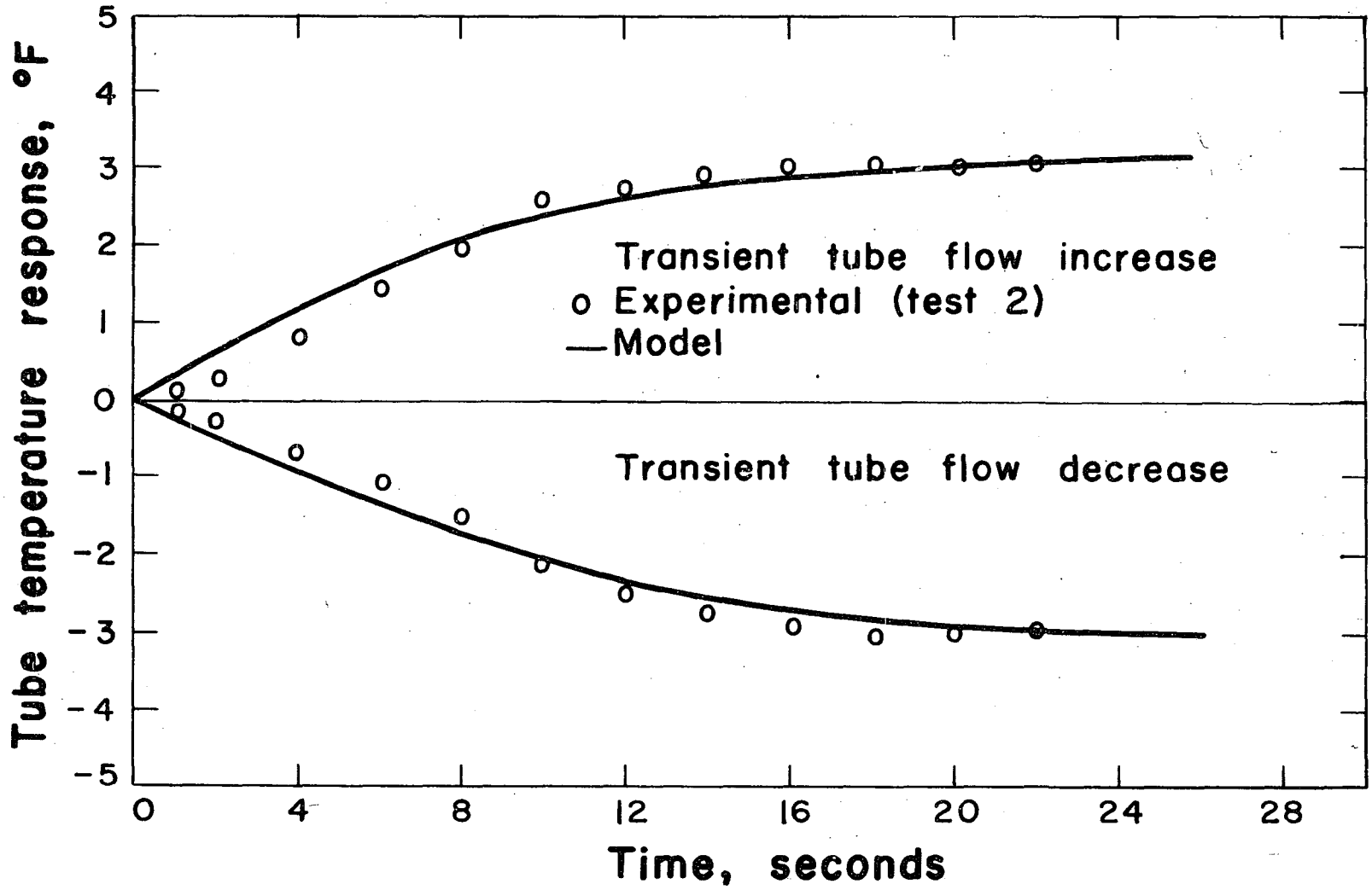
Tube temperature response, °F
5
4
3
2
1
0
-1
-2
-3
-4
-5
0
4
8
12
16
20
24
28
Time, seconds
Transient tube flow increase
o Experimental (test 2)
—Model
Transient tube flow decrease

Figure 10. Experimental transient response for Test 3 and theoretical transient response obtained using Model VII

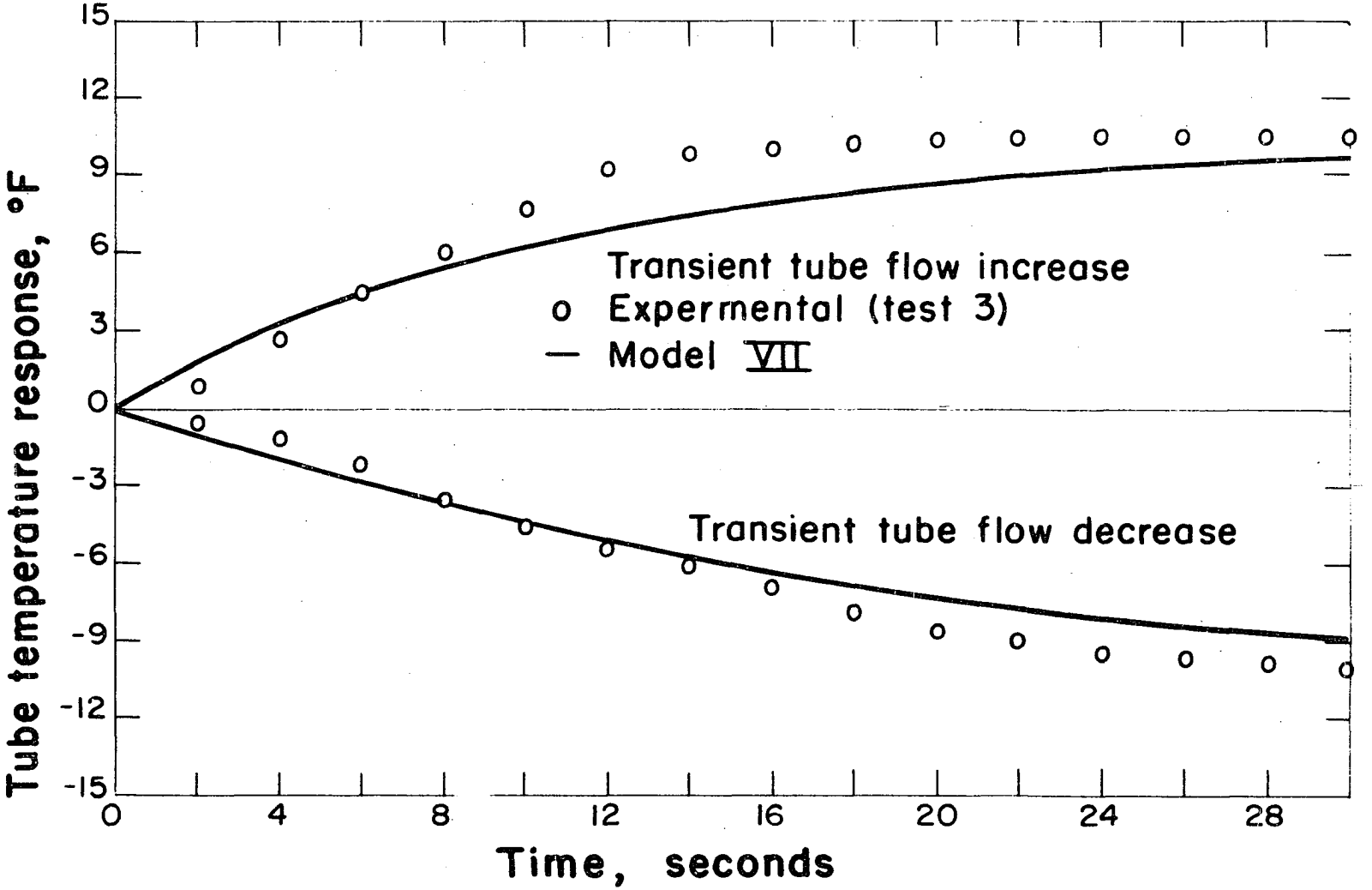
Tube temperature response, °F
15
12
9
6
3
0
-3
-6
-9
-12
-15
0
4
8
12
16
20
24
28
Time, seconds
Transient tube flow increase
o Expermental (test 3)
— Model VII
Transient tube flow decrease

Figure 11. Experimental transient response for Test 4 and theoretical transient response obtained using Model VII

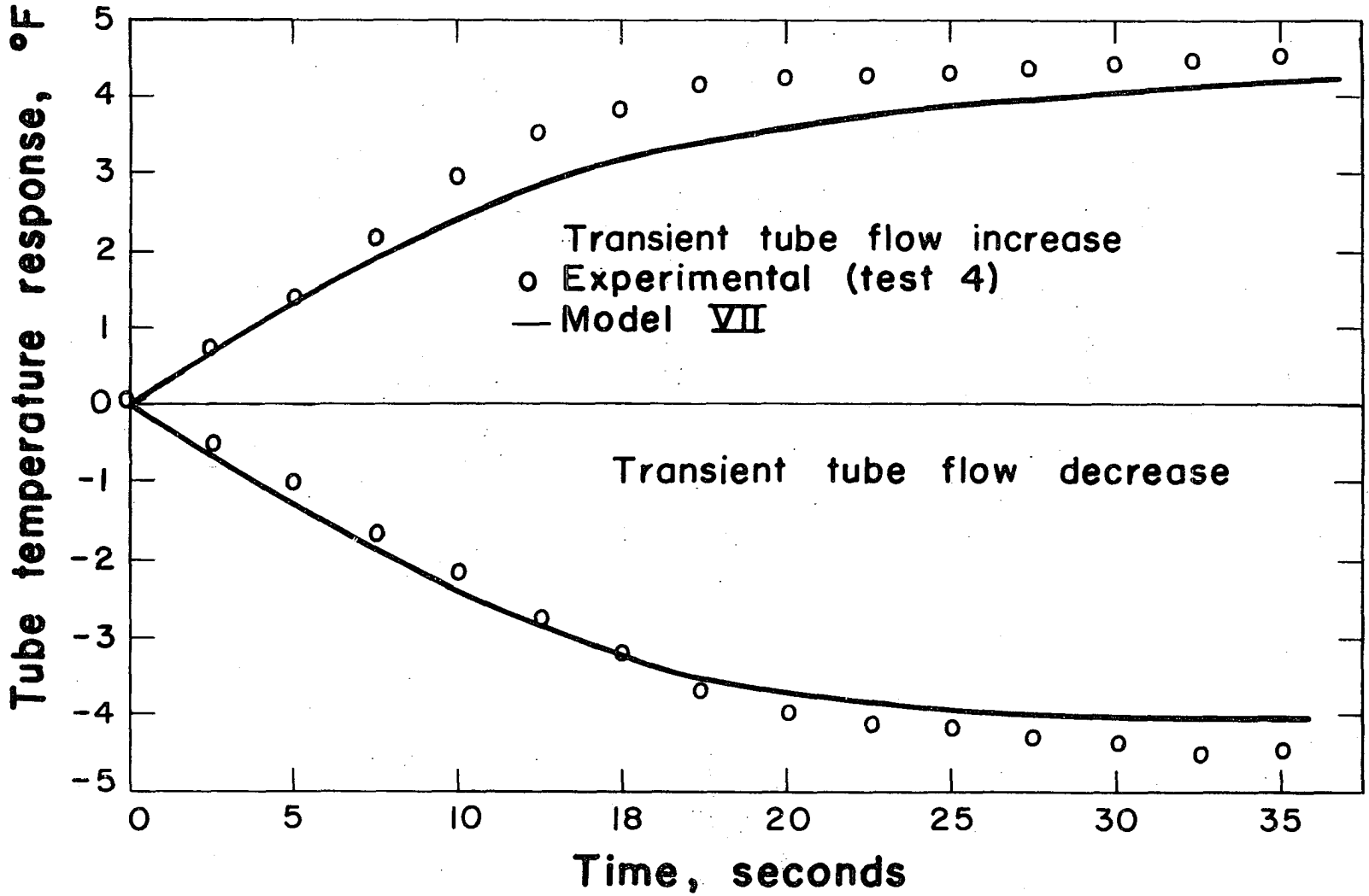
Tube temperature response, °F
5
4
3
2
1
0
-1
-2
-3
-4
-5
0
5
10
18
20
25
30
35
Time, seconds
Transient tube flow increase
o Experimental (test 4)
— Model VII
Transient tube flow decrease

Figure 12. Experimental transient response for Test 5 and theoretical transient response obtained using Model VII

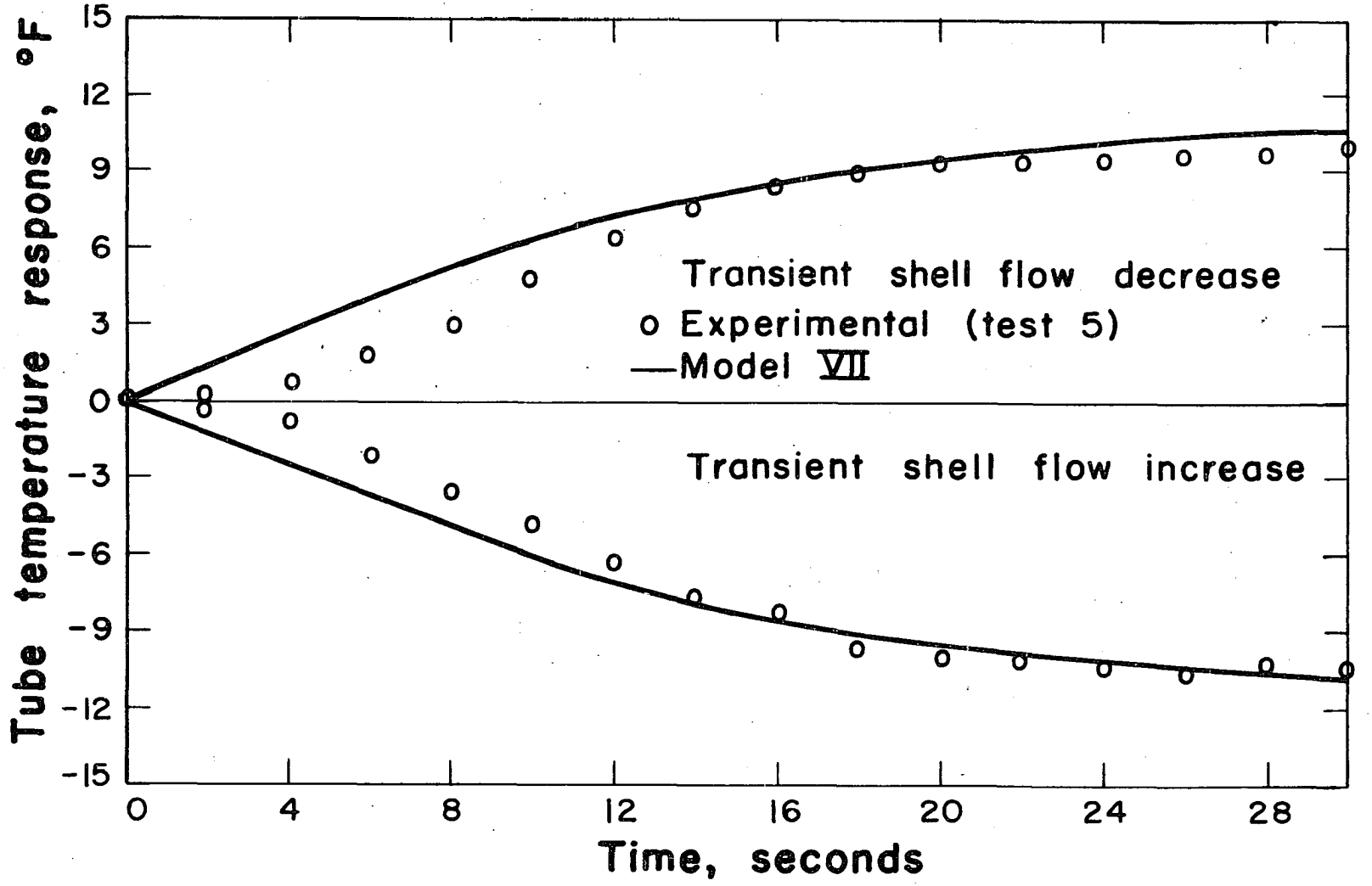
Tube temperature response, °F
15
12
9
6
3
0
-3
-6
-9
-12
-15
0
4
8
12
16
20
24
28
Time, seconds
Transient shell flow decrease
o Experimental (test 5)
—Model VII
Transient shell flow increase

Figure 13. Experimental transient response for Test 6 and theoretical transient response obtained using Model VII

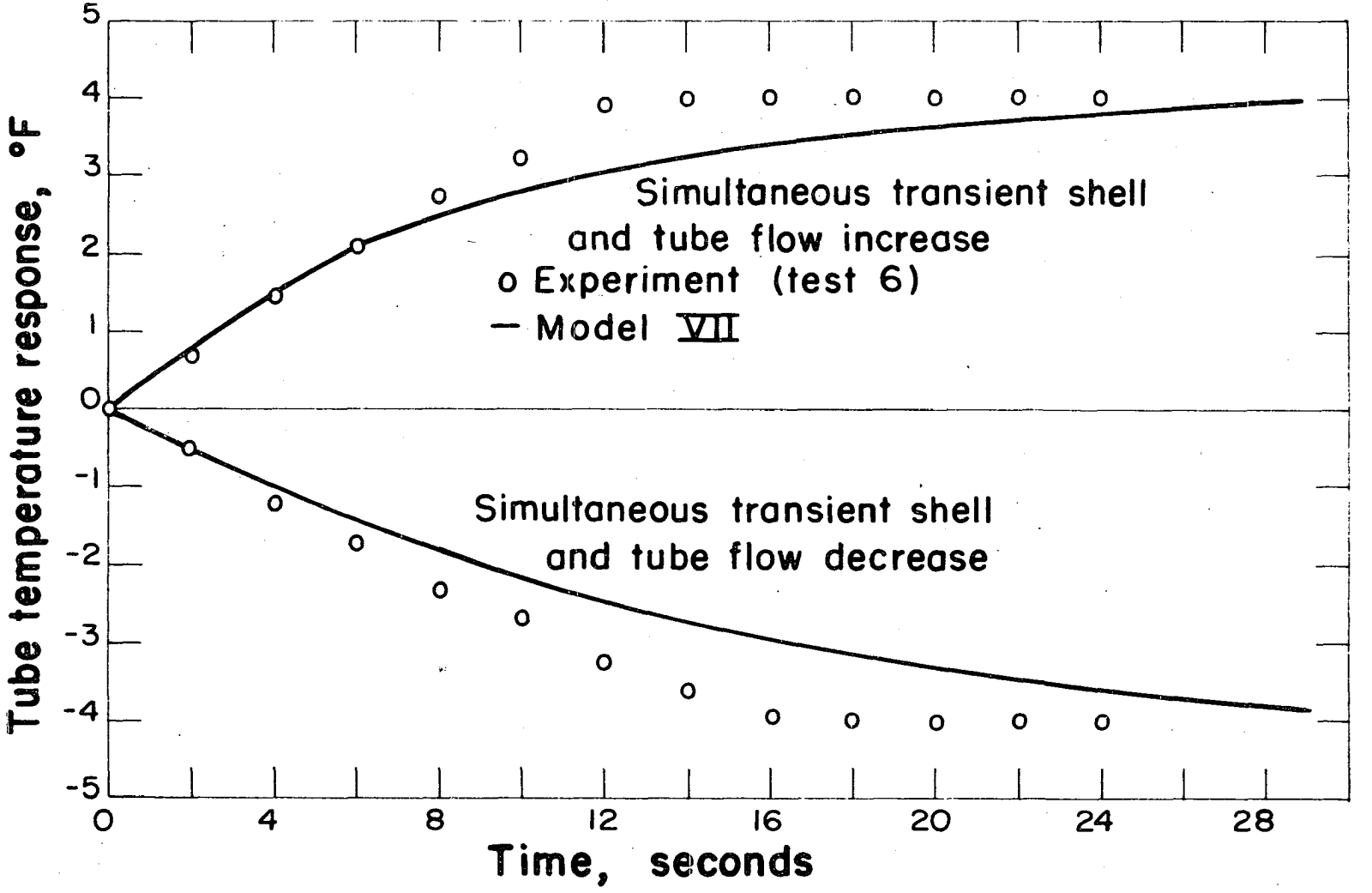
Tube temperature response, °F
5
4
3
2
1
0
-1
-2
-3
-4
-5
0
4
8
12
16
20
24
28
Time, seconds
Simultaneous transient shell
and tube flow increase
o Experiment (test 6)
— Model VII
Simultaneous transient shell
and tube flow decrease

initially as the experimental data does. The reason for this is more apparent in Models VIII and IX which are different forms of Model VII. In each of these transfer functions there are two poles and one zero indicating that the system behaves as a first order system when described by this model. This is evident from the transient response results and from the frequency response results in Figures 14 to 17 which have the characteristic first order system property of a limiting phase lag of 90°. Experimental and theoretical frequency response agreement with Model VII is good at low frequencies but very poor at high frequencies. Resonance of course is not predicted with the lumped parameter model.

Figure 14. Experimental frequency response for Test 1 and theoretical frequency response obtained using Model VIII

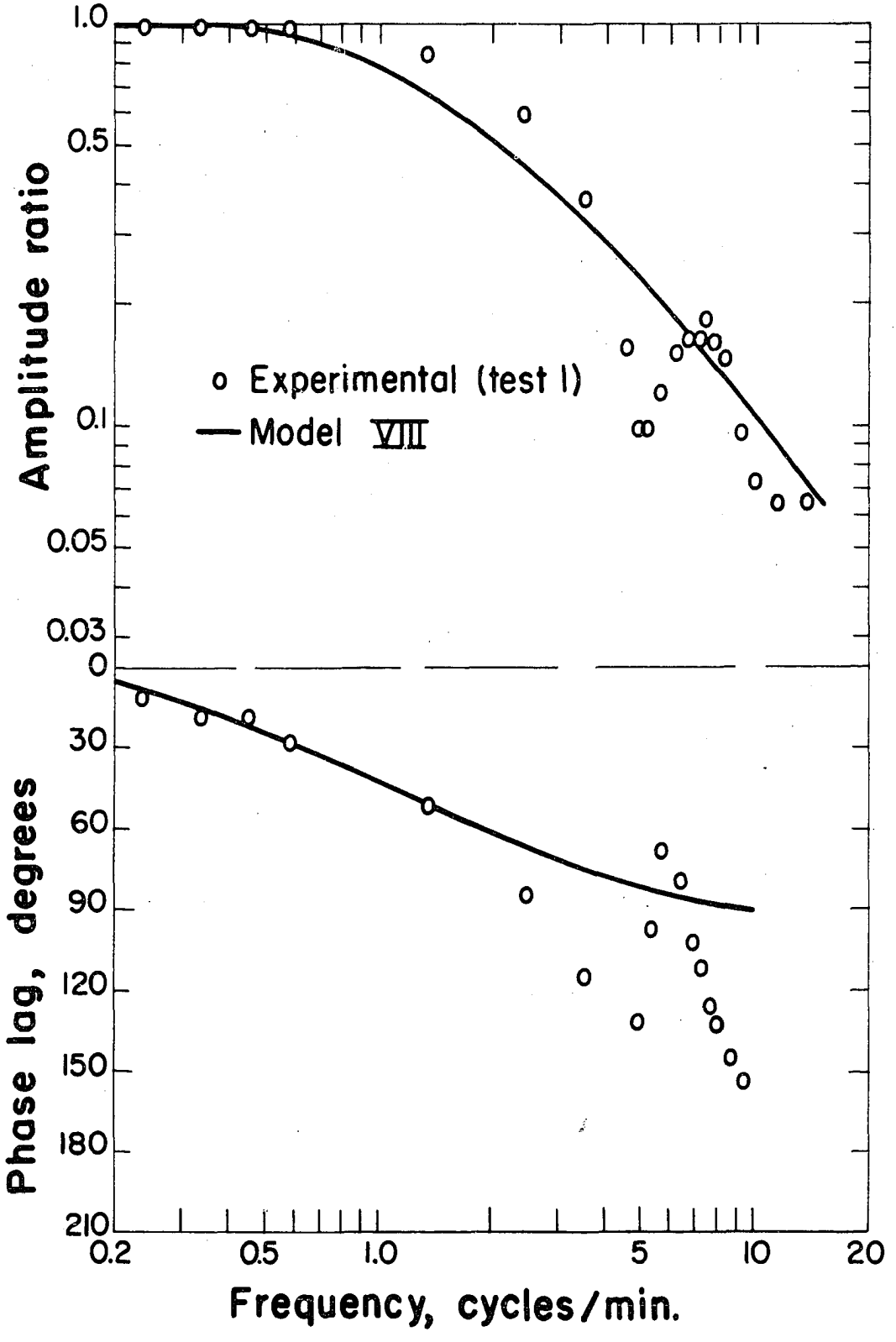
1.0
0.5
0.1
0.05
0.03
0
Amplitude ratio
o Experimental (test I)
— Model VIII
30
60
90
120
150
180
210
Phase lag, degrees
0.2
0.5
1.0
5
10
20
Frequency, cycles/min.

Figure 15. Experimental frequency response for Test 3 and theoretical frequency response obtained using Model VIII

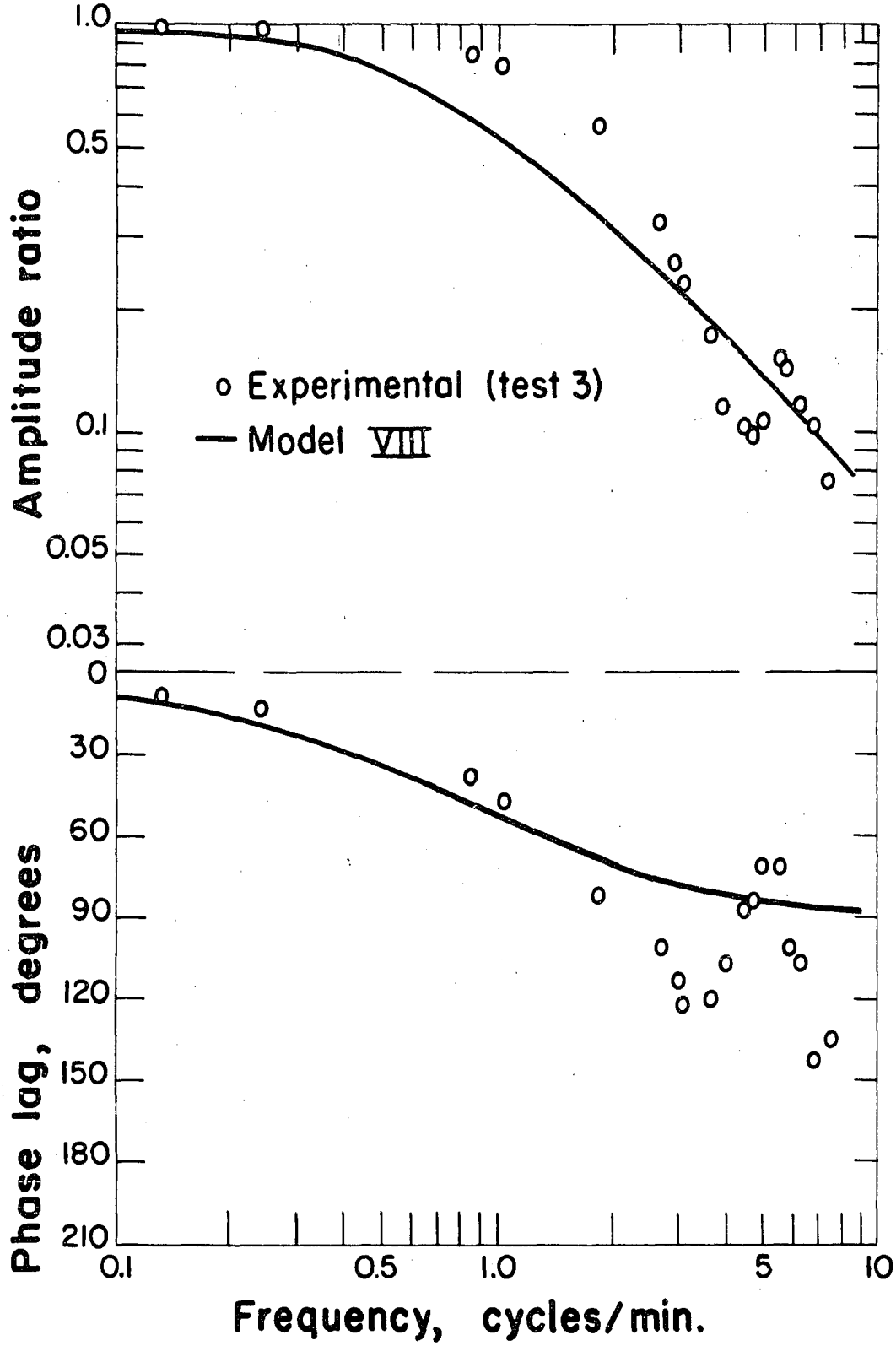
1.0
0.5
0.1
0.05
0.03
0
Amplitude ratio
o Experimental (test 3)
— Model VIII
30
60
90
120
150
180
210
Phase lag, degrees
0.1
0.5
1.0
5
10
Frequency, cycles/min.

Figure 16. Experimental frequency response for Test 5 and theoretical frequency response obtained using Model IX

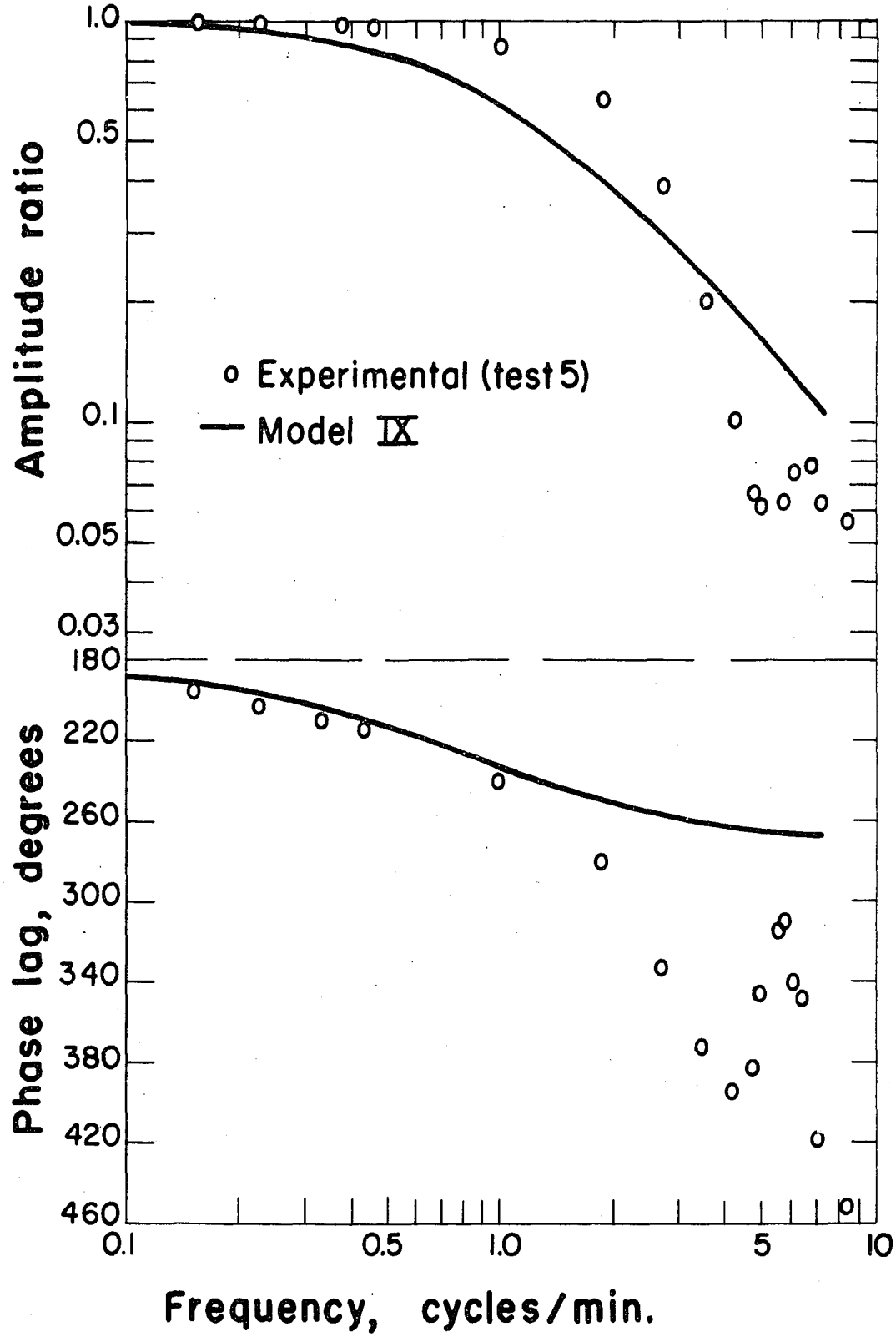
Amplitude ratio
1.0
0.5
0.1
0.05
0.03
o Experimental (test 5)
— Model IX
Phase lag, degrees
180
220
260
300
340
380
420
460
0.1
0.5
1.0
5
10
Frequency, cycles/min.

Figure 17. Experimental frequency respons for Test 6 and theoretical frequency response obtained using Model VII

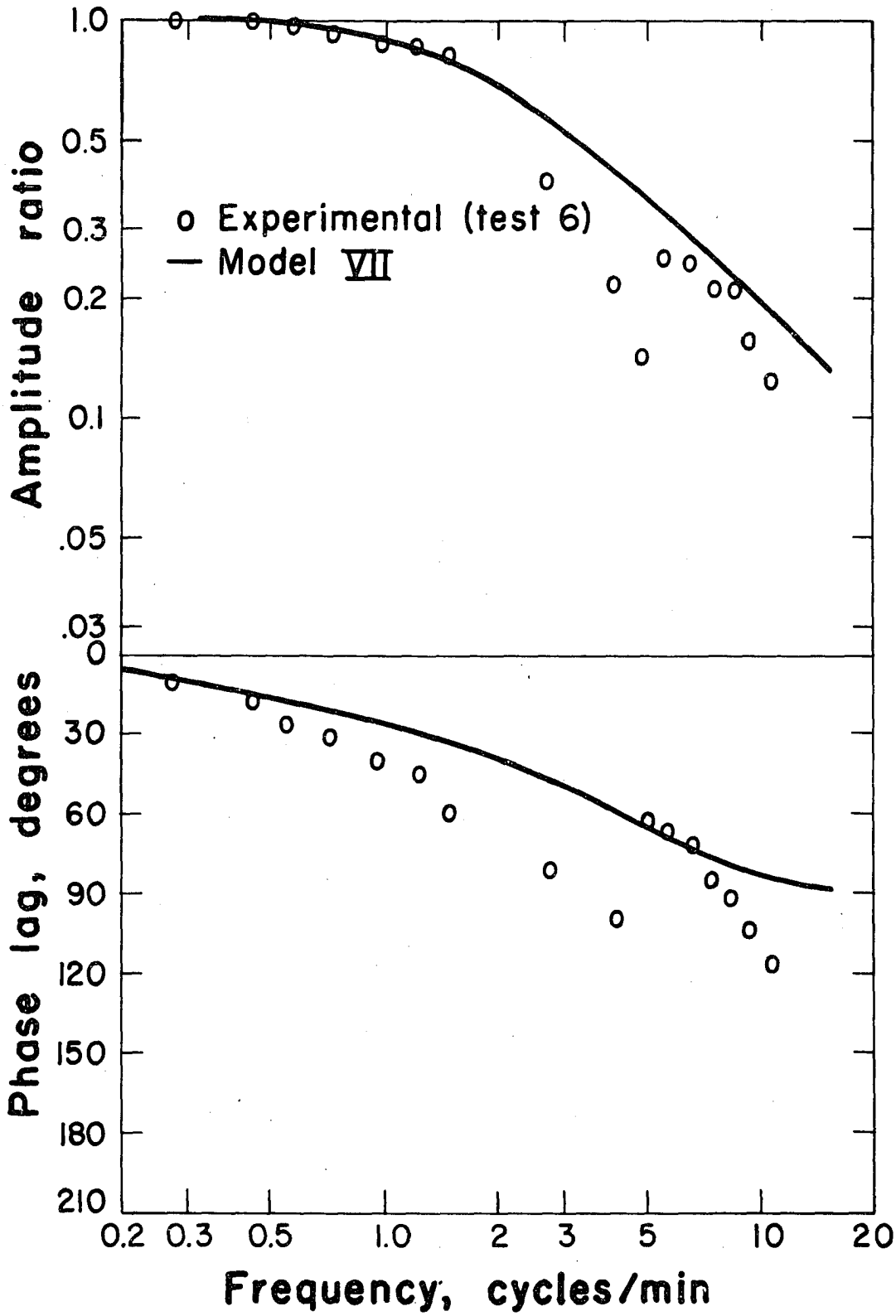
Amplitude ratio
1.0
0.5
0.3
0.2
0.1
.05
.03
o Experimental (test 6)
— Model VII
Phase lag, degrees
0
30
60
90
120
150
180
210
0.2
0.3
0.5
1.0
2
3
5
10
20
Frequency, cycles/min

CONCLUSIONS

1. Large flow upsets of 60 to 70 per cent of the mean flow rate and small flow upsets do not give significantly different experimental or theoretical frequency response results. This indicates the system behaves linearly in the range of flow perturbations investigated and that for purposes of stability analysis constant coefficient models are adequate.

2. The contribution of tube wall capacitance to the mathematical description of the system may be neglected without introducing significant error into the model. The effect of wall capacitance softens the resonance dip but does not affect the resonance frequency. Neglecting wall capacitance gives a much simpler and more useable model for describing the system dynamics than when it is included.

3. Heat transfer coefficient variation does not significantly affect frequency response results. For a nearly constant shell temperature (very high shell flow rate or steam in shell) varying the heat transfer coefficient has no effect, whereas a small effect results when heat transfer coefficient variation is considered for equal mass flow rates in the shell and tube.

4. The appropriate temperature forcing terms in the partial differential equation representation of the system

may be neglected because they are small compared to flow forcing terms. This permits relatively simple transfer functions to be derived for shell and tube upsets in flow rate. Without this assumption it would not be feasible to obtain frequency and transient response results for this system by hand calculation methods.

5. Resonance is a characteristic of distributed parameter systems and the frequency at which resonance occurs is determined by the residence time of fluid passing through the system and the upset frequency. Each stream has its own resonance frequency which occurs when $L\omega/V = 2\pi$. The type of upset, whether it is shell flow, shell temperature or tube flow, does not affect the resonance frequency, but the upset must be uniformly and simultaneously distributed along the length of the system.

6. Resonance can be controlled in systems by proper design of equipment. Combination of a long system with low flow rates causes resonance to occur at very low frequencies. Short systems with high flow rates have high resonance frequencies. The resonance frequency is calculable using $L\omega/V = 2\pi$.

7. Model IV may be applied to co-current, counter-current or constant shell temperature heat exchange by putting the proper sign on shell flow rate for each case. For co-current flow both the shell and tube flow rates have

the same sign, for counter-current flow they have opposite signs and for constant shell temperature the shell flow is considered infinite.

8. The partial differential equation models adequately represent the transient response behavior of the system for small upsets up to 25 per cent of the mean flow rate. Results are poor for larger upsets because dropping the terms involving products of perturbations introduces significant error into the final temperature change predicted. Frequency response results are not affected by large upsets because normalizing the amplitude ratios eliminates the effect of perturbation magnitude. This indicates that for simulation purposes variable coefficient models should be used to represent distributed parameter heat exchange systems when large perturbations are expected.

9. The ordinary differential equation Model VII gives good transient response results, but it predicts good frequency response results only at low frequencies. It is important to note that this model was developed using arithmetic mean fluid temperatures for heat transfer driving force terms but not in accumulation terms as Mozely (17) proposed for temperature upsets. The differential equations are developed to predict output temperature response. If the derivative with respect to time of arithmetic average temperature is used rather than the derivative of output

temperature, a model results that predicts the temperature response of the fluid in the middle of the heat exchanger. This of course is undesirable because fluid at the middle of the exchanger responds to upsets twice as fast as output fluid due to the transport time differences.

10. Transient increases and decreases in tube flow rate over the same flow range give different tube temperature response curves because tube flow rate and heat transfer coefficient variation affect the time constant of the tube fluid. Shell flow transient increases and decreases give tube temperature response curves that are nearly mirror images over the same flow range because the tube time constant does not depend directly on shell flow as it does on tube flow. Only the variation in heat transfer coefficient causes change in the tube time constant and this is small compared to the steady state time constant.

LITERATURE CITED

1. Campbell, Donald P. Process dynamics. New York, N. Y., Wiley. 1958.

2. Catheron, Allen R. and Hainsworth, Bruce D. Dynamics of liquid flow control. Industrial and Engineering Chemistry 48: 1042-1046. 1956.

3. Cima, R. M. and London, A. L. The transient response of a two-fluid counterflow heat exchanger - the gas turbine regenerator. American Society of Mechanical Engineering Transactions 82: 1169-1179. 1958.

4. Cohen, William C. and Johnson, Ernest F. Dynamic characteristics of double pipe heat exchangers. Industrial and Engineering Chemistry 48: 1031-1034. 1956.

5. Debolt, Richard R. Dynamic characteristics of a steam-water heat exchanger. Unpublished M.S. thesis. Berkeley, Calif., University of California Library. 1954.

6. Edwards, Charles L. Dynamics of a flow forced concentric tube heat exchanger. Unpublished Ph.D. thesis. Madison, Wisc., Library, University of Wisconsin. 1958.

7. Fanning, R. J. Analyze plant control by transient response. Petroleum Refiner 40, No. 3: 145-148. March, 1961.

8. Fanning, R. J. and Sliepcevich, C. M. The dynamic heat transfer characteristics of a continuous agitated tank reactor. Unpublished Ph.D. thesis. Norman, Okla., Library, University of Oklahoma. 1958.

9. Ford, R. L. Electrical analogues for heat exchangers. Institute of Electrical Engineers Proceedings 103, Part B: 65-82. 1956.

10. Gilliland, E. R., Gould, L. A. and Rinard, I. H. A series method for the analysis of plug flow process dynamics, Part I. (Mimeographed) Boston, Mass. Department of Chemical Engineering, Massachusetts Institute of Technology. 1961.

11. Hainsworth, B. D., Tivy, V. V. and Paynter, H. M. Dynamic analysis of heat exchanger control. Instrument Society of America Journal 4: 230-235. June, 1957.

12. Hempel, Arvid. On the dynamics of steam-liquid heat exchangers. American Society of Mechanical Engineering Transactions 82: 244-251. 1961.

13. Iscol, Lewis. Frequency response of shell and tube heat exchangers. Unpublished Ph.D. thesis. Madison, Wisc., Library, University of Wisconsin. 1959.

14. Koppel, Lowell B. Dynamics of a flow-forced heat exchanger. Industrial and Engineering Chemistry Fundamentals 1, No. 2: 131-134. 1962.

15. Lees, Sydney and Hougen, Joel O. Pulse testing a model heat exchange process. Industrial and Engineering Chemistry 48: 1064-1068. 1956.

16. Morris, H. J. The dynamic response of shell and tube heat exchangers to temperature disturbances. (Mimeographed) St. Louis, Mo., Res. and Eng. Div., Monsanto Chemical Co. 1959.

17. Mozely, J. M. Predicting dynamics of concentric pipe heat exchangers. Industrial and Engineering Chemistry 48: 1035-1041. 1956.

18. Paynter, H. M. and Takahashi, Y. A new method of evaluating dynamic response of counter-flow and parallel-flow heat exchangers. American Society of Mechanical Engineering Transactions 78: 749-758. 1956.

19. Rizika, J. W. Thermal lags in flowing systems containing heat capacitors. American Society of Mechanical Engineering Transactions 78: 1412-1418. 1956.

20. Rizika, J. W. Thermal lags in flowing systems containing heat capacitors. American Society of Mechanical Engineering Transactions 76: 411-420. 1954.

21. Smith, Otto J. M. Feedback control systems. New York, N. Y., McGraw-Hill. 1958.

22. Stermole, F. J. Dynamic response of heat exchangers to flow rate changes. Unpublished M.S. thesis. Ames, Iowa, Library, Iowa State University of Science and Technology. 1961.

23. Stermole, F. J. and Larson, M. A. Dynamic response of heat exchangers to flow rate changes. Industrial Chemistry Fundamentals 2: 62-67. 1963.

24. Takahashi, E. Y. Transfer function analysis of heat exchange processes. In Tustin, A. Automatic and manual control. pp. 235-248. New York, N. Y., Academic Press. 1952.

25. Wilt, Charles H. Principles of feedback control. London, England, Addison-Wesley. 1960.

26. Yang, W. J., Clark, J. A. and Arpaci, V. S. Dynamic response of heat exchangers having internal heat sources - Part IV. American Society of Mechanical Engineering Transactions Ser. C, 83: 321-338. 1961.

NOMENCLATURE

A	cross sectional area, ft^2
C	heat capacity, BTU/lb ^oF
h	heat transfer film coefficient, BTU/sec ft^2 ^oF
k	unit less constant relating flow changes to heat transfer coefficient changes
L	heat exchanger length, ft
P_s	outside perimeter of tube, ft
P_t	inside perimeter of tube, ft
p	Laplace transform operator for length, ft^{-1}
s	Laplace transform operator for time, sec^{-1}
t	time, sec
U	overall heat transfer coefficient, BTU/sec ft^2 ^oF
$\mathcal{U}$	unit function
V	fluid velocity, ft/sec
W	mass flow rate, lb/min
x	axial distance coordinate, ft
ρ	density, lb/ft^3
θ	temperature, ^oF
ω	frequency, cycles/min or rad/sec

Subscripts

i	initial steady state value
L	at axial distance x = 0

0 at axial distance x = L

s refers to shell or fluid in shell

t refers to tube or fluid in tube

w tube wall

Superscripts

' deviation from initial steady state value

- Laplace transformed variable with respect to time

= Laplace transformed variable with respect to both time and distance

ACKNOWLEDGMENTS

The author wishes to express his gratitude to Dr. Maurice A. Larson for his guidance and assistance during the course of this investigation and to the Iowa Engineering Experiment Station for the financial support of this project.

APPENDIX

Table 2. Experimental frequency response data for output tube water temperature response to sinusoidal flow rate changes

ω cycles/min	Amp. ratio	Phase lag(^{o})	ω cycles/min	Amp. ratio	Phase lag(^{o})
	Test 1			Test 2	
.235	1.00	10	.194	1.00	9
.333	1.00	16	.267	1.00	12
.445	.990	17	.387	.992	20
.570	.980	26	.521	.968	20
1.32	.850	50	1.26	.859	38
2.40	.600	83	2.35	.632	70
3.43	.375	113	3.48	.410	125
4.50	.160	149	4.72	.133	140
4.80	.104	130	5.00	.122	97
5.21	.100	94	5.45	.160	56
5.55	.125	67	5.88	.180	62
6.25	.158	79	6.31	.205	93
6.66	.167	100	6.60	.215	95
7.07	.167	110	7.06	.205	125
7.45	.190	125	7.75	.184	144
7.80	.167	130	8.75	.112	153
8.28	.150	144	10.9	.081	-
9.10	.100	153			
10.0	.075	-			
11.4	.067	110			
13.2	.067	-			

Table 2. (Continued)

ω cycles/min	Amp. ratio	Phase lag(°)	ω cycles/min	Amp. ratio	Phase lag(°)
	Test 3			Test 4	
.136	1.00	8	.112	1.00	7
.245	1.00	13	.292	1.00	22
.860	0.848	38	.414	.965	30
1.05	0.805	47	.521	.931	33
1.84	0.572	82	.800	.887	48
2.70	0.331	101	1.43	.743	77
3.00	0.267	113	2.07	.576	104
3.16	0.238	123	2.79	.326	129
3.64	0.178	120	3.75	.182	135
4.00	0.117	108	4.14	.152	120
4.45	0.104	87	4.70	.174	104
4.70	0.092	85	5.15	.235	95
5.05	0.108	71	6.31	.182	133
5.55	0.150	70	7.00	.136	150
5.82	0.145	103	7.85	.091	175
6.31	0.117	107			
6.75	0.104	142			
7.50	0.075	135			

Table 2. (Continued)

ω cycles/min	Amp. ratio	Phase lag(°)		ω cycles/min	Amp. ratio	Phase lag(°)
	Test 5				Test 6	
.154	1.00	16	196	.279	1.00	10
.228	.991	22	202	.462	1.00	18
.333	.972	30	210	.572	.972	27
.429	.954	35	215	.727	.943	31
1.00	.865	60	240	.976	.887	41
1.85	.631	100	280	1.50	.815	59
2.70	.390	154	334	2.79	.393	84
3.53	.203	191	371	4.14	.214	99
4.20	.100	214	394	5.00	.143	63
4.80	.068	202	382	5.61	.257	67
5.00	.061	165	345	6.60	.257	77
5.71	.063	137	317	7.60	.210	86
5.88	.063	134	314	8.35	.210	91
6.15	.075	162	342	9.50	.157	104
6.60	.078	168	348	10.9	.128	118
7.09	.063	238	418			
8.34	.056	275	455			